Check for updates

Secretin activates brown fat and induces satiation

Sanna Laurila[1,2,3], Lihua Sun[1,20], Minna Lahesmaa[1,4,20], Katharina Schnabl[5,6,7], Kirsi Laitinen[8], Riku Klén[1], Yongguo Li[5,6,7], Miroslav Balaz[9], Christian Wolfrum[9], Katja Steiger[10], Tarja Niemi[11], Markku Taittonen[12], Mueez U-Din[1,13], Tommi Välikangas[14], Laura L. Elo[8,14,15], Olli Eskola[1], Anna K. Kirjavainen[1], Lauri Nummenmaa[1,16], Kirsi A. Virtanen[13,17,18], Martin Klingenspor[5,6,7] and Pirjo Nuutila[1,13,19] ✉

Brown adipose tissue (BAT) thermogenesis is activated by feeding. Recently, we revealed a secretin-mediated gut–BAT–brain axis, which stimulates satiation in mice, but the purpose of meal-induced BAT activation in humans has been unclear. In this placebo-controlled, randomized crossover study, we investigated the effects of intravenous secretin on BAT metabolism (measured with [18F]FDG and [15O]H₂O positron emission tomography) and appetite (measured with functional magnetic resonance imaging) in healthy, normal weight men (GUTBAT trial no. NCT03290846). Participants were blinded to the intervention. Secretin increased BAT glucose uptake (primary endpoint) compared to placebo by 57% (median (interquartile range, IQR), 0.82 (0.77) versus 0.59 (0.53) µmol per 100 g per min, 95% confidence interval (CI) (0.09, 0.89), P = 0.002, effect size r = 0.570), while BAT perfusion remained unchanged (mean (s.d.) 4.73 (1.82) versus 6.14 (3.05) ml per 100 g per min, 95%CI (−2.91, 0.07), P = 0.063, effect size d = −0.549) (n = 15). Whole body energy expenditure increased by 2% (P = 0.011) (n = 15). Secretin attenuated blood-oxygen level-dependent activity (primary endpoint) in brain reward circuits during food cue tasks (significance level false discovery rate corrected at P = 0.05) (n = 14). Caloric intake did not significantly change, but motivation to refeed after a meal was delayed by 39 min (P = 0.039) (n = 14). No adverse effects were detected. Here we show in humans that secretin activates BAT, reduces central responses to appetizing food and delays the motivation to refeed after a meal. This suggests that meal-induced, secretin-mediated BAT activation is relevant in the control of food intake in humans. As obesity is increasing worldwide, this appetite regulating axis offers new possibilities for clinical research in treating obesity.

During the past ten years, human brown adipose tissue (BAT) has emerged as a potential therapeutic target for metabolic dysfunction and obesity[1]. BAT activity has been shown to negatively associate with insulin resistance and obesity in humans[2,3], but the effect of BAT thermogenesis on human energy balance seems to be limited by the relatively small mass of BAT found in humans[4]. It has thus been proposed that BAT has beneficial effects on other metabolically active organs through neuronal and hormonal mechanisms beyond mere energy dissipation[5,6].

Meal-associated BAT thermogenesis occurs in mice[7,8] and in humans[9], but its physiological function and relevance have been unclear. A link between BAT activation and appetite suppression has been suggested by indirect evidence in previous studies. Mild cold-induced BAT activation is associated with lower serum ghrelin concentrations[10] and a thermogenic meal is associated with a sensation of fullness[11]. In 2018, we reported that the gut hormone secretin mediates meal-associated BAT thermogenesis and thereby induces satiation in mice[12]. We observed that secretin receptors (SCTR) were abundantly expressed in murine BAT[12]. Feeding increased circulating secretin levels, which on binding to SCTR in

brown adipocytes initiated lipolysis and ignited uncoupling protein 1 (UCP1)-dependent thermogenesis[12], and inhibited feeding[12]. In humans, BAT thermogenesis correlated with the postprandial rise in serum secretin levels[12]. Since this new satiation promoting gut–BAT–brain axis may explain some of the metabolic benefits of BAT in humans, we aimed to investigate this mechanism further with a placebo-controlled crossover study, using positron emission tomography (PET) combined with computed tomography to study BAT activation (n = 15) and functional magnetic resonance imaging (fMRI) to study appetite (n = 14) (Fig. 1 and Extended Data Fig. 1).

Results

Secretin-driven human BAT activation. To further investigate the role of secretin in humans, we conducted a placebo-controlled crossover study, in which intravenous infusions of secretin hydrochloride and saline were given to 15 healthy males in the fasting state (Fig. 1a). Study participants were blinded to the intervention. PET/CT was used to measure BAT perfusion and BAT glucose uptake (GU) during the infusions. We first used [15O]H₂O (radiowater) to quantify BAT perfusion during the first 6 min. Thereafter,

[1]Turku PET Centre, University of Turku, Turku, Finland. [2]Heart Center, Turku University Hospital, Turku, Finland. [3]Satakunta Central Hospital, Pori, Finland. [4]Department of Internal Medicine, Jorvi Hospital, Helsinki University Hospital, Helsinki, Finland. [5]Chair for Molecular Nutritional Medicine, Technical University of Munich, TUM School of Life Sciences, Freising, Germany. [6]EKFZ - Else Kröner Fresenius Center for Nutritional Medicine, Technical University of Munich, Freising, Germany. [7]ZIEL – Institute for Food & Health, Technical University of Munich, Freising, Germany. [8]Institute of Biomedicine, University of Turku, Turku, Finland. [9]Institute of Food, Nutrition and Health, ETH Zürich, Schwerzenbach, Switzerland. [10]Institue of Pathology, School of Medicine, Technical University of Munich, Munich, Germany. [11]Department of Plastic and General Surgery, Turku University Hospital, Turku, Finland. [12]Department of Anesthesiology, Turku University Hospital, Turku, Finland. [13]Turku PET Centre, Turku University Hospital, Turku, Finland. [14]Turku Bioscience Centre, University of Turku, Turku, Finland. [15]Turku Bioscience Centre, Åbo Akademi University, Turku, Finland. [16]Department of Psychology, University of Turku, Turku, Finland. [17]Institute of Public Health and Clinical Nutrition - University of Eastern Finland (UEF), Kuopio, Finland. [18]Department of Endocrinology and Clinical Nutrition, Kuopio University Hospital, Kuopio, Finland. [19]Department of Endocrinology, Turku University Hospital, Turku, Finland. [20]These authors contributed equally: Lihua Sun, Minna Lahesmaa. ✉e-mail: pirjo.nuutila@utu.fi
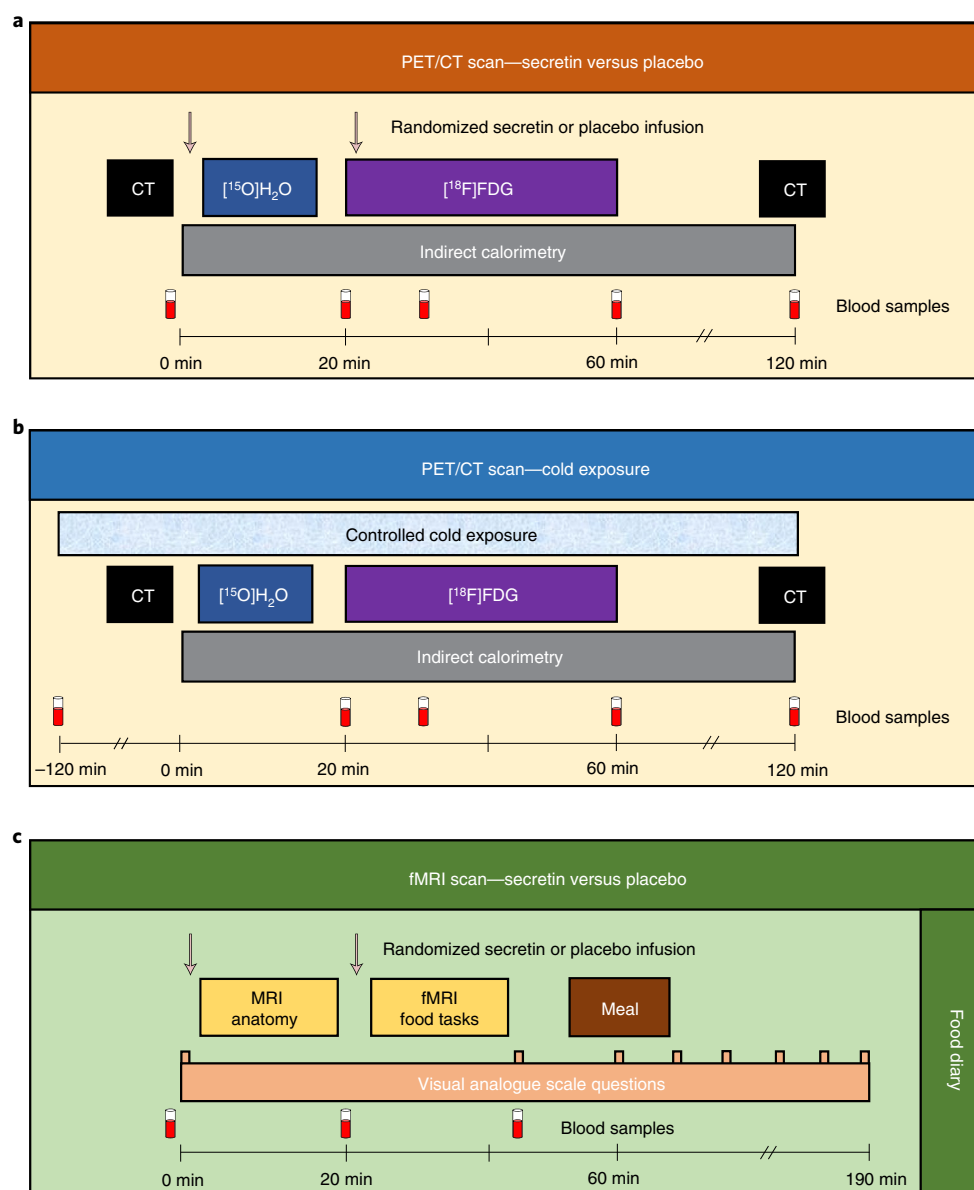
Fig. 1 | Study protocol. a,b, Participants ($n=15$) underwent three PET/CT scans: two at room temperature (**a**) and one during controlled cold exposure (**b**). Participants were randomized to receive secretin and placebo infusions on separate days, during room temperature scans. Infusions were given twice. **c**, Participants ($n=14$) underwent two fMRI scans, where they were also randomized to receive secretin and placebo infusions on separate days. After scanning, participants had a meal and were then followed up for 2 h. Subjective measurements on appetite were collected with VAS questionnaires (Extended Data Fig. 2) at prespecified time points. **a–c**, All scans were conducted in the morning after an overnight fast.

GU was quantified using [18F]FDG, the gold standard method for investigating BAT activation in humans. Our aim was to time the [18F]FDG scan for highest BAT activation.

Statistics of paired outcome measures are shown in Table 1. We found that secretin increases BAT GU compared to placebo (median (IQR) secretin versus placebo, 0.82 (0.77) µmol per 100 g per min versus 0.59 (0.53) µmol per 100 g per min, $P=0.002$) (Fig. 2c,d), in line with our previous report[12]. Secretin increased BAT GU, even when an apparent outlier was excluded from analysis ($n=14$, median (IQR) secretin versus placebo, 0.80 (0.65) µmol per 100 g per min versus 0.59 (0.49) µmol per 100 g per min, $P=0.003$). The difference between interventions for the whole group was also significant when analysed with a fixed effect model ($F_{2,15}=6.937$, $P=0.020$). We tested for covariates and found that body-mass index (BMI), age, homeostatic model assessment for insulin resistance

(HOMA-IR) and oral glucose insulin sensitivity (OGIS) did not contribute to the result (BMI, $F_{2,15}=9.979$, $P=0.950$), age ($F_{2,15}=3.474$, $P=0.245$), HOMA-IR ($F_{2,15}=0.027$, $P=0.871$ and OGIS ($F_{2,15}=0.085$, $P=0.775$)). This was expected, as all our participants were healthy and had normal insulin sensitivity.

Along with metabolic activation of BAT, skeletal muscle GU was also higher after secretin infusion (mean (s.d.) secretin versus placebo, 1.21 (0.48) µmol per 100 g per min versus 0.81 (0.22) µmol per 100 g per min, $P=0.003$) (Extended Data Fig. 3a). This suggests a close interaction of BAT and muscles after secretin stimulation, which is also seen during cold exposure[13]. According to the Online Biology Gene Portal System (BioGPS)[14], SCTRs are also expressed in human skeletal muscle[15] (Extended Data Fig. 3b). BAT perfusion remained unchanged when measured within the first 6 min of the infusion (mean (s.d.) secretin versus placebo, 4.73 (1.82) ml per 100 g per min

Table 1 | Statistics on paired outcome measures

Outcome measure	Secretin	Placebo	95% CI	P value	Effect size
	Mean (s.d.)	Mean (s.d.)			
BAT GU (µmol per 100 g per min)	1.16 (0.69)	0.67 (0.36)	0.09, 0.89	0.002[a]	0.570[b]
Muscle GU (µmol per 100 g per min)	1.21 (0.48)	0.81 (0.22)	0.16, 0.63	0.003	0.942
BAT perfusion (ml per 100 g per min)	4.73 (1.82)	6.14 (3.05)	−2.91, 0.07	0.063	−0.549
Whole body energy expenditure (kcal d⁻¹)	1,689.89 (161.46)	1,643.56 (138.66)	12.39, 80.29	0.011	0.788
Whole body oxygen consumption (ml min⁻¹)	244.69 (23.60)	238.41 (20.34)	0.86, 11.70	0.026	0.669
AUC CCS preprandial	49.68 (18.23)	41.37 (18.23)	1.10, 15.52	0.027	0.665
AUC CCS preprandial + prandial	91.18 (36.95)	75.88 (35.70)	3.64, 26.97	0.014	0.757
AUC CCS postprandial	311.33 (136.08)	266.15 (126.42)	−15.27, 105.63	0.130	0.432
AUC CCS all	430.94 (179.28)	366.75 (164.02)	−6.68, 135.05	0.072	0.523
Meal size (kcal)	488.97 (109.42)	522.00 (167.45)	−95.31, 29.25	0.273	−0.306
Resumption to eat (min)	260.77 (86.45)	222.15 (66.89)	2.23, 75.00	0.039	0.641

A table showing statistics of paired outcome measures reported in this paper. Mean values, s.d., 95% CI, P values for paired samples t-test and Cohen's d for effect size are shown. All paired tests were two-sided. [a]Wilcoxon signed-rank test. [b]Effect size r calculated as $r = Z/\sqrt{N}$, where Z is Z-score, and N is number of observations. Abbreviations: composite satiety score, CCS; area under the curve, AUC.

versus 6.14 (3.05) ml per 100 g per min, $P=0.063$) (Extended Data Fig. 3c). In our previous study with mice, maximal BAT thermogenesis was reached after 20 min of secretin administration[12]. There is no immediate effect, as the hormone needs to first be distributed in the body and cellular processes such as lipolysis are required for UCP1 activation[12]. It is therefore likely that BAT thermogenesis is initiated at a later time point in humans as well and an increase in perfusion could not be observed with this study design. Furthermore, serum secretin concentrations increased after secretin infusions to physiological levels attained during a postprandial phase[12] (Fig. 2a,b), but due to the rapid half-life of secretin hydrochloride, the peaks were brief. More prolonged and higher BAT activation may be possible to observe with a longer acting secretin analogue, but unfortunately there are none on the market for human use.

Additionally, we measured energy expenditure using indirect calorimetry measurements during the PET/CT scan, to further study whole body metabolism. We found that secretin increases whole body energy expenditure (mean (s.d.) secretin versus placebo, 1,690.0 (161.5) kcal d⁻¹ versus 1,643.6 (138.7) kcal d⁻¹, $P=0.011$) (Fig. 2e). This in itself may indicate thermogenesis and it is likely that other tissues contribute to it in addition to BAT. This thermogenic effect was based on a mild increase in whole body oxygen consumption ($\dot{V}O_2$) after secretin administration (mean (s.d.) secretin versus placebo, 244.7 (23.6) ml min⁻¹ versus 238.4 (20.3) ml min⁻¹, $P=0.026$). This shows that secretin may have potential as a catabolic agent.

Secretin increases satiation in humans. We previously demonstrated the neurobiological basis of secretin's BAT to brain satiation effect in mice, using hypothalamic biopsies[12]. To further analyse the central effects and scrutinize the direct link between BAT thermogenesis and appetite, we here applied fMRI, using a previously established method[16] (Fig. 1c). Fourteen male participants conducted food cue tasks, where pictures of palatable versus non-palatable foods were shown to engage the reward circuit and appetitive mechanisms, for example, similar to when seeing pictures of food in advertisements (Fig. 3a). The timing of the fMRI sequence was adjusted to the timing of the [¹⁸F]FDG PET/CT BAT scan for us to study BAT GU and appetite at identical time points.

We found that secretin lowered the responses to palatable food images. In the placebo condition, viewing palatable versus non-palatable foods increased hemodynamic brain activity in the medial frontal cortex, cingulate cortex, caudate and middle and posterior insula, similar to previous studies[16]. This anticipatory reward-sensitive coding of the food images was abolished after the secretin infusion (Fig. 3b). Interaction effects between food categories and conditions were found in the reward circuits. Therefore, secretin essentially abolished the differential coding of palatable versus non-palatable foods in the brain reward circuits. These effects were unchanged when participants with the largest head motions were initially included (Extended Data Fig. 4a).

We also studied satiety during the study days by CSS[17], calculated from visual analogue scale (VAS) questions (Extended Data Fig. 2). Secretin increased subjective satiety compared to placebo in fasting conditions (mean (s.d.) AUC secretin versus placebo, 49.7 (18.2) versus 41.4 (18.2), $P=0.027$) and during early feeding (mean (s.d.) AUC secretin versus placebo, 91.2 (37.0) versus 75.9 (35.7), $P=0.014$), but not postprandially (mean (s.d.) AUC secretin versus placebo, 311.3 (136.1) versus 266.2 (126.4), $P=0.130$) (Fig. 4a–c and Extended Data Fig. 4b,c). This finding is in line with our earlier study, where we found that secretin decreases the food intake of wild type mice in prandial and early postprandial, but not in the late postprandial phase[12].

Secretin's effect on calorie intake was investigated by providing a standardized meal after the fMRI scan and allowing participants to eat until satiated. Food diaries were also used. Although the meal size was numerically smaller after secretin compared to placebo, the difference was not statistically significant (mean (s.d.) secretin versus placebo, 489.0 (109.4) kcal versus 522.0 (167.5) kcal, $P=0.273$). The study was underpowered for this exploratory outcome and a larger sample size will be needed in future studies to determine whether secretin decreases meal size. However, secretin delayed resumption to eat after the test meal, with a mean delay of 39 min compared to the placebo (mean (s.d.) secretin versus placebo, 260.8 (86.5) min versus 222.2 (66.9) min, $P=0.039$) (Fig. 4d). According to 6-d food diaries, there were no statistically significant differences in daily dietary intakes during the study (Supplementary Table 1).

SCTR gene expression and regulation in BAT. In mice, *SCTR* is abundantly expressed in BAT and the gut hormone directly activates BAT thermogenesis, independent of efferent sympathetic innervation[12]. This was shown in our previous study in mice by administration of propranolol, which inhibits sympathetic activation. Propranolol did not attenuate secretin induced BAT thermogenesis[12]. Since cold-induced activation is initiated through the sympathetic nervous system, we conducted a cold exposure
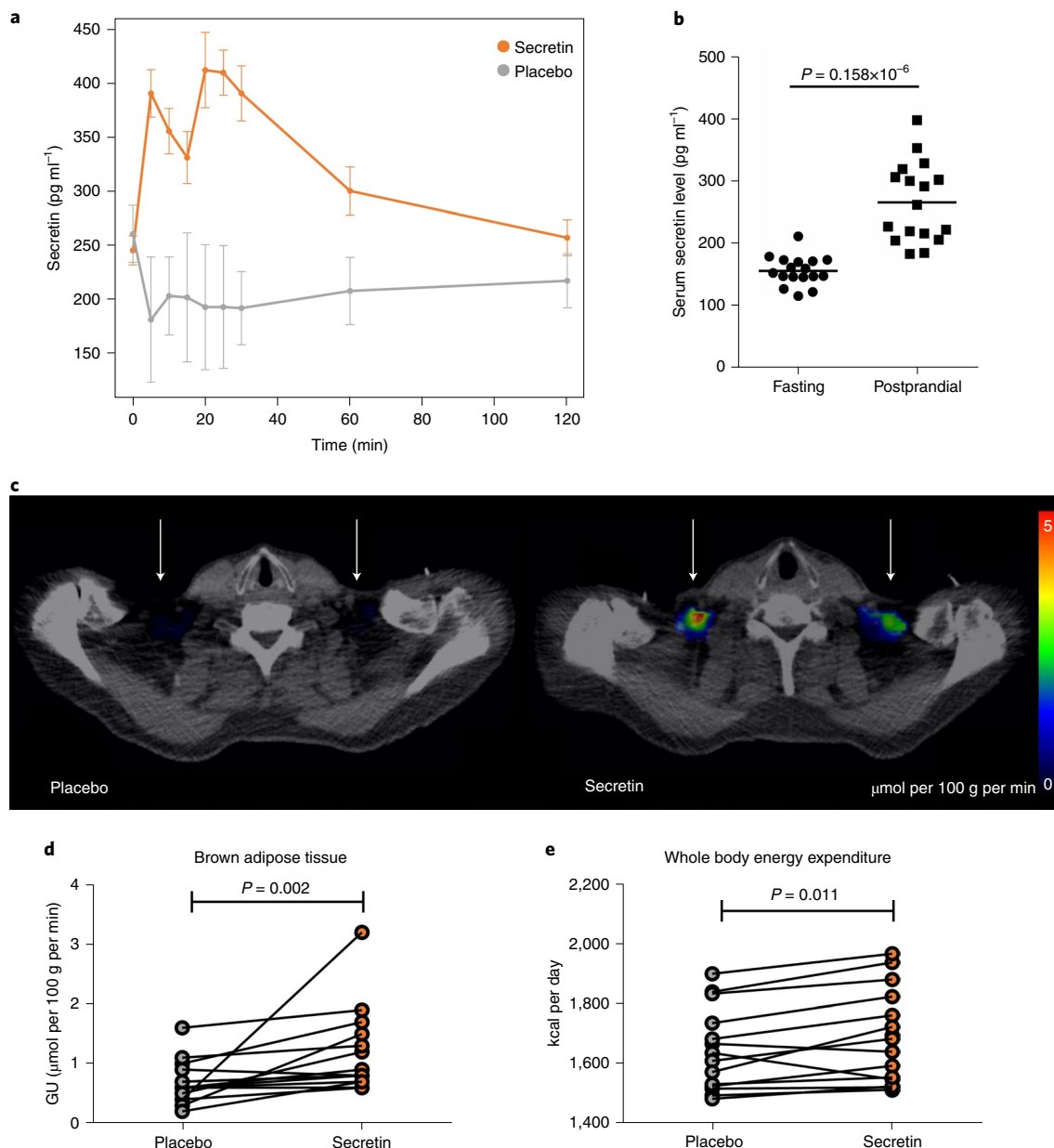
Fig. 2 | Secretin increases GU in human BAT. a, Secretin pentahydrochloride (1 IU kg⁻¹) given at 0 and 20 min increased serum secretin levels for the duration of the [¹⁸F]FDG PET/CT scan. Mean secretin levels and standard error are shown for n = 14 during the secretin and n = 5 during the placebo intervention. No statistical analysis is shown on the graph, as secretin was mainly measured for the quality control of secretin pentahydrochloride administration. **b**, Serum secretin levels in fasting and postprandial participants, reported in our previous study[12] (n = 17). **c**, Representative parametric [¹⁸F] FDG PET/CT images from supraclavicular BAT (n = 1). Arrows indicate the location of BAT. **d**, The effect of secretin infusion on GU in BAT compared to placebo (n = 15). n = 6 of the datapoints were reported in our previous study[12]. The increase in BAT GU by secretin is significant even when the apparent outlier is excluded (Supplementary Information). **e**, The effect of secretin infusion on whole body energy expenditure, compared to placebo (n = 15). **b,d**, Data were analysed by two-sided paired Wilcoxon signed-rank test, due to the non-normality of the differences. **e**, Data were analysed by a two-sided paired samples t-test.

scan (n = 15) to compare these effects (Fig. 1b). Cold-induced BAT GU was increased compared to room temperature (placebo condition) (n = 15, median (IQR) cold versus room temperature, 2.36 (8.06) µmol per 100 g per min versus 0.599 (0.51) µmol per 100 g per min, P = 0.003), in line with previous studies[1]. There was no association between cold-induced BAT GU and secretin induced BAT GU, which further supports our hypothesis of direct BAT activation through SCTR in humans (r = −0.107 (−0.554, 0.466), P = 0.704) (Extended Data Fig. 5a).

To validate our hypothesis of secretin's direct ability to activate human BAT, we obtained image-guided BAT biopsies from study participants for SCTR identification by immunohistochemistry. SCTR was detected in all five human BAT biopsies studied (Fig. 5a). Staining of SCTR was mainly localized to the cytoplasm and the cell membranes of adipocytes. Neurons were negative for SCTR, whereas some staining was found in non-adipocytes, most probably endothelial cells. In adipocytes, SCTR staining intensity and frequency was heterogeneous.
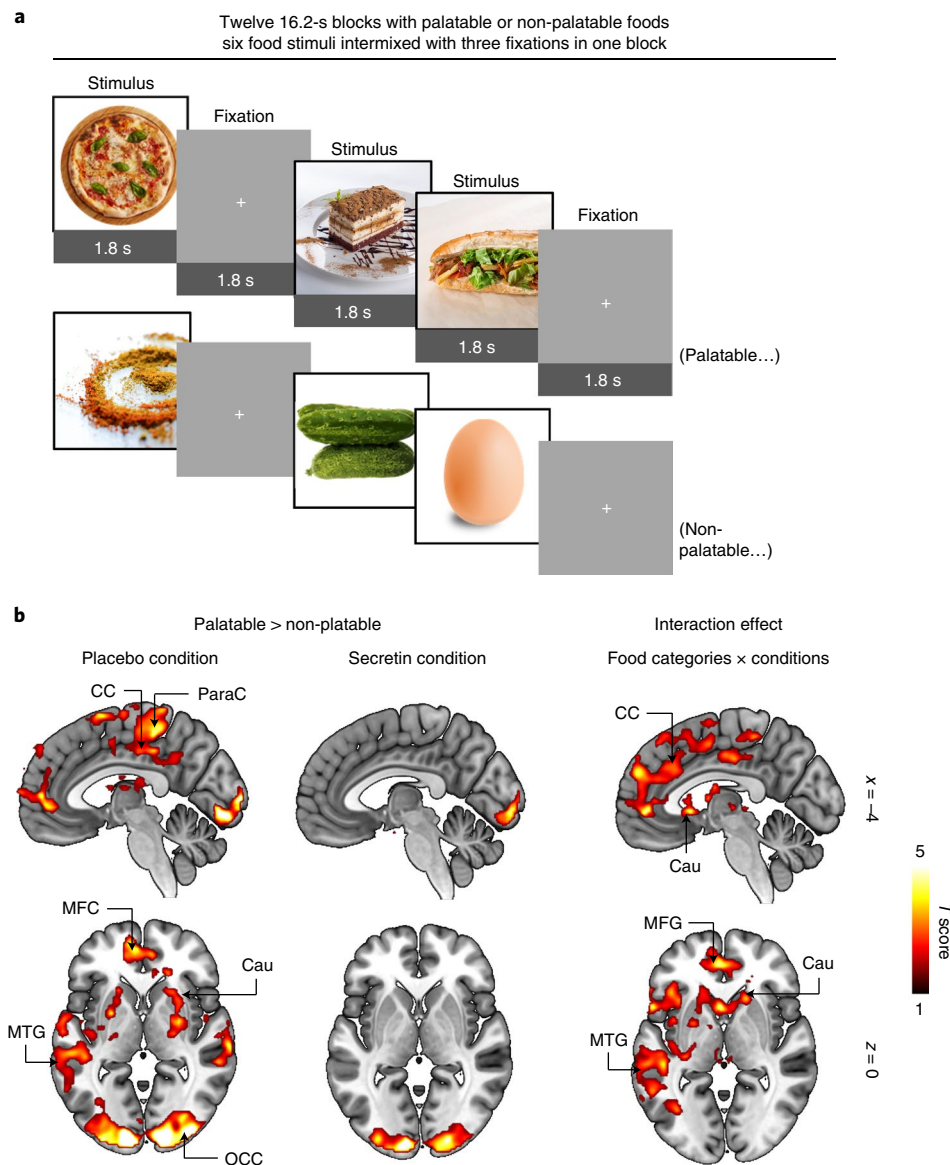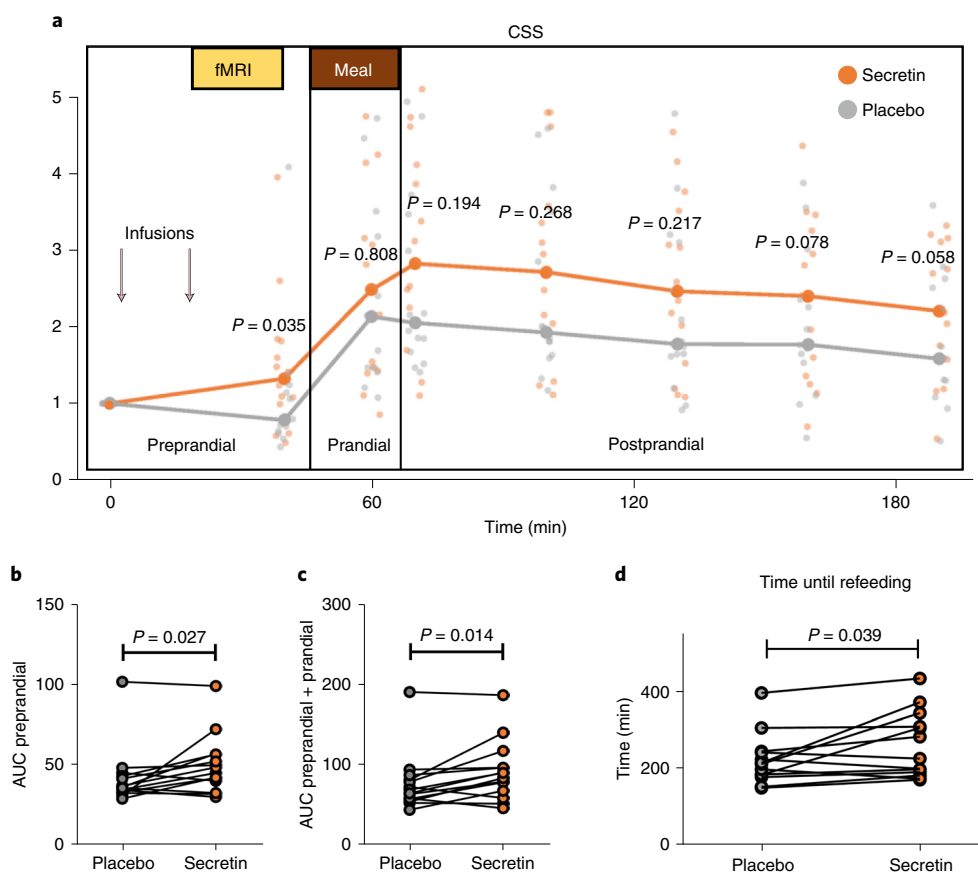
Fig. 3 | Secretin induces satiation when measured by fMRI. Downregulated brain reward anticipation response due to injection of secretin ($n = 11$).
a, fMRI model where pictures of palatable versus non-palatable foods were presented to participants under secretin or placebo conditions. **b**, In the placebo condition, viewing palatable versus non-palatable foods increased BOLD activity in brain reward circuits. This effect was diminished in the secretin condition. Interaction effect between food categories and drug conditions were found in the same regions, indicating secretin-dependent changes. Significance level was false discovery rate corrected at $P = 0.05$. All statistical parametric images (including the effect size maps) can be found from NeuroVault at https://neurovault.org/collections/ECURNRON/. Findings remained when including participants with large movement artefacts ($n = 14$) (Extended Data Fig. 4a). MFC, medial frontal cortex; CC, cingulate cortex; OCC, occipital cortex; Cau, caudate and MTG, middle temporal gyrus.

We confirmed *SCTR* gene expression on the messenger RNA level in two independent cohorts from previously reported studies with human participants[9,18]. Notably, we found a negative correlation of *SCTR* mRNA levels in BAT with body mass ($r = −0.678$, $P = 0.008$) (Fig. 5b) and a weak negative association with body-mass-index ($r = −0.470$, $P = 0.090$) (Extended Data Fig. 5b). An association of *SCTR* gene expression and body weight was only observed in participants who had fasted before biopsy, while there was no association in non-fasted participants (body mass $r = −0.120$, $P = 0.684$, and BMI $r = −0.235$, $P = 0.418$) (Fig. 5c, Extended Data Fig. 5c). The absence of an association between both parameters in non-fasted participants is most probably due to meal-induced downregulation of *SCTR* expression by its ligand secretin, as revealed by our analyses in mice. Comparison of mice in the fasted and fed state

revealed that elevated serum secretin levels in the fed state are associated with downregulation of *Sctr* (mean (s.d.) relative mRNA level (Sctr/Gtf2b), fasted ($n = 6$) versus fed ($n = 6$), 6.16 (2.00) versus 2.60 (3.36), $P = 0.045$) (Fig. 5d). Furthermore, secretin treatment decreased *Sctr* mRNA levels in primary murine brown adipocytes in a dose-dependent manner (Fig. 5e).

Secretin's effect on hormone and metabolite levels. To further examine the metabolic effects of secretin, we also studied serum samples during secretin and placebo scans. Serum non-esterified fatty acid (NEFA) levels were elevated by secretin for the duration of the [18F]FDG PET/CT scan (Fig. 6a). Previous studies have shown that secretin activates lipolysis[19,20]. Although the increased systemic NEFA levels probably originate from white adipose tissue due to its

Fig. 4 | Secretin induces satiation when measured by CSS. a–c, CSS increased after secretin compared to placebo in fasting state (**a**), and by AUC in the preprandial (**b**) and prandial (**c**) phases. **d**, A standardized meal was provided at the study centre, after which participants kept a food diary. According to self-reporting, secretin delayed resumption to eat. **a–c**, The graphs include all $n=14$ participants and **d**, $n=13$ due to missing food diary data. Data are presented as medians and standard errors or individual values. **a–c**, Values are normalized, dividing by the value of the first time point. **a**, Data were analysed by two-sided paired Wilcoxon signed-rank test. **b–d**, Data were analysed by a two-sided paired samples *t*-test.

high volume, lipolysis is known to be important not only in fuelling BAT thermogenesis but also in initiating it[13].

Earlier, we showed in mice that secretin induced BAT lipolysis ignites UCP1 coupled thermogenesis[12]. To investigate BAT fatty acid metabolism, we estimated the triglyceride content of BAT by analysing Hounsfield units (HU) from PET/CT images and calculated whole body fatty acid oxidation from indirect calorimetry measurements. Computed tomography radiodensity correlates with BAT triglyceride content measured by magnetic resonance spectroscopy (^{1}H-MRS); the higher the radiodensity of BAT, the lower the intracellular triglyceride content[21,22]. In this study, BAT radiodensity increased 2 h after secretin administration, reflecting a decrease in stored triglycerides. During the secretin scan, this change positively correlated with fat oxidation, measured by indirect calorimetry ($r=0.568$ (0.106, 0.814), $P=0.022$) (Fig. 6b). No correlation was found during the placebo scan ($r=-0.477$ (−0.873, 0.145), $P=0.085$) (Fig. 6c). When compared with Dunn and Clark's *z*-test, the correlations between BAT HU and fat oxidation were significantly different under secretin and placebo conditions ($z=2.141$, $P=0.032$). This indicates that secretin may activate human BAT thermogenesis through lipolysis stimulation, as shown in mice[12].

Insulin concentrations were increased transiently (Fig. 6e), which was reflected by a slight decrease in plasma glucose (Fig. 6d). This effect was brief and may be a response to increased lipolysis[23,24]. There may also be a synergistic effect with insulin and secretin during feeding, where intracellular BAT lipolysis is initiated by secretin, while lipolysis is simultaneously suppressed by insulin on a systemic

level. More studies are needed to confirm this. There was no correlation between insulin levels and BAT or muscle GU (Supplementary Table 2).

Secretin is known to induce bile secretion into the duodenal lumen[25] and bile acids are known to activate BAT[26]. We examined serum bile acid levels to control for this effect and saw no increase by secretin compared to placebo (Extended Data Fig. 6a). Plasma thyroid-stimulating hormone (TSH) decreased 2 h after the first secretin infusion (Extended Data Fig. 6b and Supplementary Table 3). This may indicate a role of the hypothalamic-pituitary-thyroid axis in appetite regulation[27], or it may be a compensatory effect due to increased BAT thermogenesis and T4 conversion to active T3 in BAT[28,29].

Discussion

The results of our translational study indicate that the appetite regulating gut–BAT–brain axis, shown by us previously in mice[12], is also present in healthy humans. We demonstrate that secretin induces brown fat activation and increases whole body energy expenditure, acting as a catabolic agent. This effect is relatively minor compared to cold exposure, a familiar and powerful BAT activator[1–3]. However, our results also support a regulatory role for BAT in energy homeostasis.

We show that secretin attenuates appetite and that resumption to eat is delayed after a meal. We detected SCTRs in human BAT and showed that their expression is tightly controlled by nutritional state. Cold-induced BAT GU was not associated with secretin induced GU, further supporting a direct activation mechanism
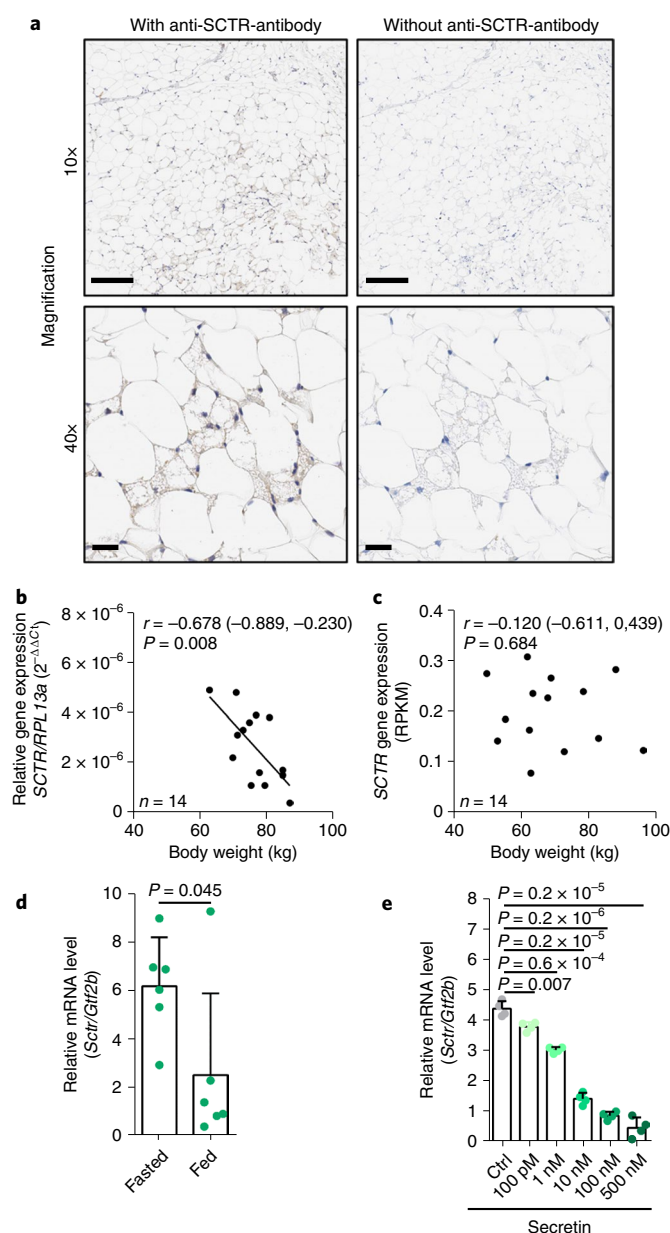
Fig. 5 | SCTR expression in BAT negatively correlates with body weight in fasted participants. a, Representative immunohistochemical detection of SCTR in human supraclavicular BAT (nuclei stain haematoxylin; magnifications ×10 and ×40; scale bars, 200 μm (upper) and 30 μm (lower)) (n = 1). **b**, SCTR expression on mRNA level, assessed by qPCR, in supraclavicular BAT is negatively associated with body weight in fasted participants (n = 14). **c**, SCTR expression analysed by RNA-Seq does not correlate with body weight in non-fasted participants (n = 14). RPKM, reads per kilobase of transcript, per million mapped reads. **d**, Sctr is downregulated in ad libitum fed mice (n = 6) compared to fasted ones (n = 6). **e**, Secretin treatment decreased Sctr mRNA levels in primary murine brown adipocytes (n = 4). **b,c**, Data were analysed by Pearson's correlation. **d,e**, Data were analysed by a two-sided unpaired t-test. ***P < 0.001, **P < 0.01, *P < 0.05. Data are presented as means and s.d.

through the SCTR. We even found indications of secretin induced BAT lipolysis, which we showed in our previous study to be important in secretin-initiated BAT thermogenesis[12].

This appetite regulating gut–BAT–brain axis has important implications for obesity and brown adipose research. Our findings

reveal a new metabolically beneficial role for BAT, possibly explaining the long elusive role of meal-induced BAT activation. Obesity is rapidly increasing worldwide[30] and this appetite regulating axis offers new possibilities for clinical research. Future clinical trials are needed to confirm whether preprandial administration of secretin has potential in decreasing food intake.

Methods

Study design. We investigated the effects of intravenous secretin infusions on BAT metabolism and appetite in this placebo-controlled, randomized crossover study, where participants were blinded to the intervention. According to the manufacturer's instructions, secretin hydrochloride must be administered immediately after preparation, due to its short half-life. Thus, we prepared the solution on location right before administration and, as such, those conducting the study could not be reliably blinded to the intervention.

The primary endpoints of the first part of the trial were BAT GU and perfusion, measured with [^{18}F]FDG and [^{15}O]H$_2$O PET, respectively. Whole body energy expenditure, measured by indirect calorimetry, was a secondary endpoint. For the second part of the study, the primary endpoint was anticipatory brain reward responses to palatable and non-palatable food images, measured by fMRI. CSS, measured by VAS questions, and calorie intake, were secondary endpoints. Image-guided BAT biopsies were obtained for SCTR identification (exploratory endpoint) and blood samples were collected during both studies (exploratory endpoint). All imaging studies were conducted at the Turku PET Centre.
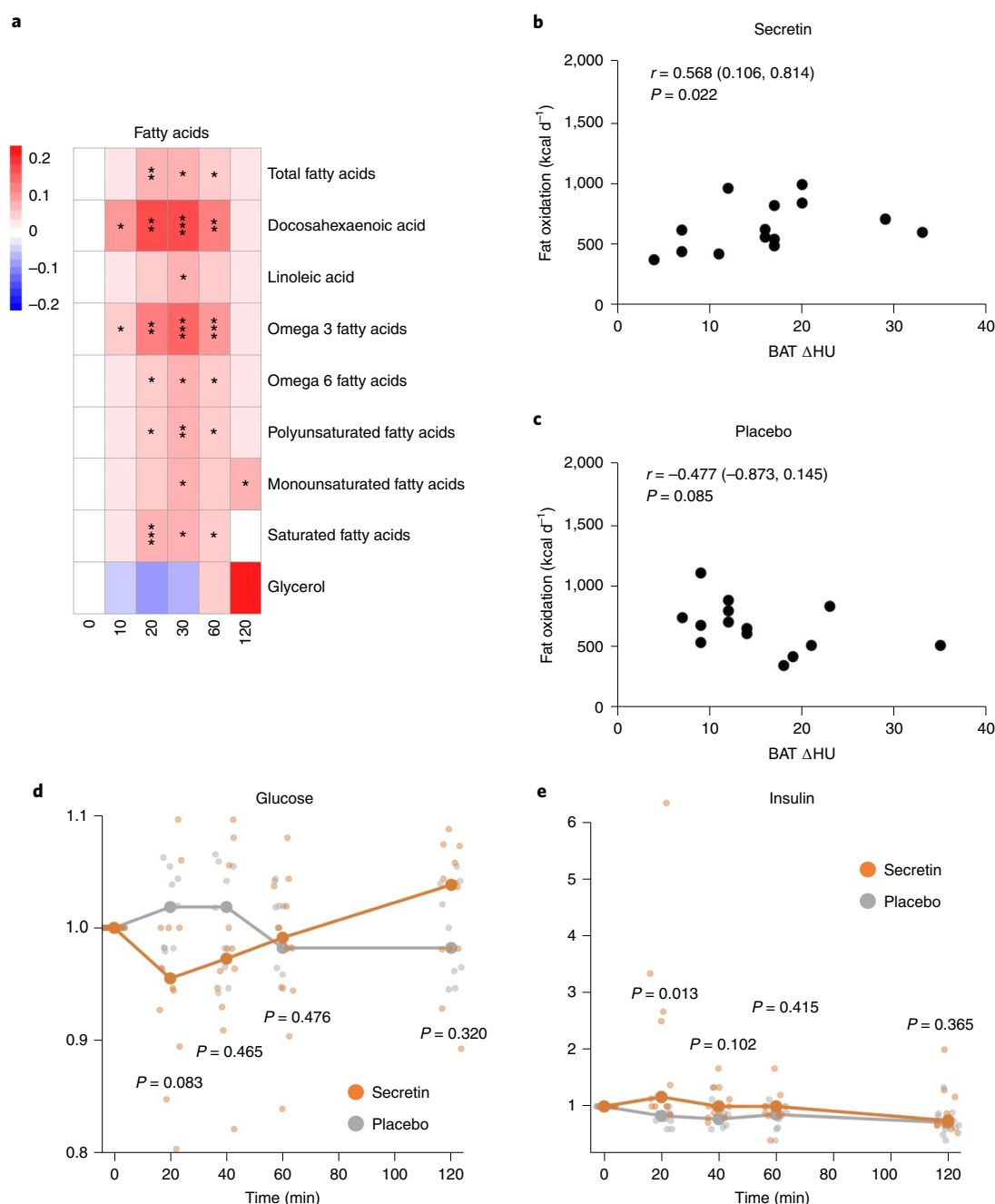
The first part of the study consisted of three PET scans performed on three separate days after an overnight fast (Fig. 1a,b). The scans on each individual were performed within 2–30 d (median 15 d), to minimize the effects of seasonal climate variation on BAT activity within each participant[31,32]. PET/CT scans were performed throughout the year. In total, 15 male participants (mean (s.d.), aged 41.6 (12.1) years, BMI 24.0 (1.9) kg m^{-2}) were included in the analysis. One of the three scans was performed during controlled cold exposure, which was started 2 h before the scan, using cooling blankets (Blanketrol III, Cincinnati Sub-Zero) as described previously[33]. Two scans were conducted at room temperature, where participants were blinded to the intervention and randomized to receive intravenous infusions of placebo (saline) and secretin (secretin pentahydrochloride 1 IU kg^{-1} × 2, Secrelux, Sanochemia) on separate days. Whole body energy expenditure was assessed with indirect calorimetry during PET scans, as described previously[33]. Blood samples were collected before and during the scans.

The second part of the study consisted of two fMRI scans, performed on two separate days in the morning after an overnight fast (Fig. 1c). Again, the individual scans were performed within 7–30 d (median 14.5 d), to minimize seasonal effects on appetite and BAT function. A total of 14 male participants (mean (s.d.), aged 34.4 (14.6) years, BMI 23.3 (1.8) kg m^{-2}) were included in the analysis. Satiety was assessed by measuring CSS by VAS questions during scan days. Participants were offered a standardized meal after each fMRI scan, and the amount of food eaten was documented at the study centre. Participants filled in food diaries 2 d before, during and 3 d after the study day.

Study approval and trial registration. The study protocol was reviewed and approved by the Ethics Committee of the Hospital District of Southwest Finland. The PET/CT trial was prospectively registered in the EudraCT registry 2 June 2016 (EudraCT no. 2016-002373-35). However, due to a human error, the registration was not initially made public. The error was corrected by the Finnish Medicines Agency (Fimea) and our registration was made public 12 August 2020. A major amendment to the trial, which introduced the fMRI study on appetite, was accepted by the Ethics Committee of the Hospital District of Southwest Finland 24 October 2017. The fMRI study was prospectively registered to Clinical Trials 25 September 2017, together with a retrospective registration of the PET/CT trial (Clinical Trials no. NCT03290846). The study was not industry sponsored.

Study participants. A total of n = 21 healthy men (n = 21, mean (s.d.), age 35.2 (14.4) years, BMI 23.6 (1.9) kg m^{-2}) provided data for analysis; n = 15 with PET combined with computed tomography (PET/CT) and n = 14 with fMRI (Extended Data Fig. 1). A group of 16 participants was recruited for the PET/CT study. One participant discontinued his participation in the study after one scan and was excluded from analysis. After the PET/CT study, 11 participants provided written informed consent for the fMRI study. An additional group of six participants was recruited with the same inclusion and exclusion criteria. Data from one participant was excluded from analysis due to considerable protocol deviations and from two participants due to a technical failure of the MRI scanner. Six participants gave additional consent to obtain supraclavicular BAT biopsies. One participant was excluded from analysis due to insufficient sample quality. All participants were recruited between the years 2016 and 2018. The trial ended when all preplanned studies were completed. No notable harm or unintended effects were observed.

All enrolled participants (n = 22) met the inclusion criteria and presented healthy at the screening visit. Inclusion criteria included BMI 20–26 kg m^{-2}, male sex and age 18–65 years. Exclusion criteria included any chronic disease (such as diabetes) or medication (such as steroids, beta blockers or asthma medications)

a

Fatty acids

b Secretin

r = 0.568 (0.106, 0.814)
P = 0.022

c Placebo

r = −0.477 (−0.873, 0.145)
P = 0.085

d Glucose

P = 0.083
P = 0.465
P = 0.476
P = 0.320

Secretin
Placebo

e Insulin

Secretin
Placebo

P = 0.013
P = 0.102
P = 0.415
P = 0.365

Fig. 6 | Secretin changes circulating metabolite and hormone levels. a, Secretin increased serum NEFA levels for the duration of the PET/CT scan. **b,c**, Whole body fat oxidation correlates with an increase in BAT radiodensity after secretin (**b**), but not after placebo (**c**). **d,e**, Glucose was initially decreased (**d**) as insulin levels briefly increased (**e**). For changes in other measured carbohydrates, see Extended Data Fig. 6c. **a,d,e**, Values were normalized, dividing by the value of the first time point (*n* = 12). Each time point was analysed by two-sided paired Wilcoxon signed-rank test. **P* < 0.05, ***P* < 0.01, ****P* < 0.001. **b,c**, Data were analysed by Spearman's rank correlation to avoid assumptions around linearity of associations (*n* = 15). **d,e**, Median values and standard error are shown on graphs. Exact *P* values for the presented heatmaps are listed in Supplementary Table 3.

that would affect the outcome or safety (such as excessive alcohol use or a history of pancreatitis) of the study and currently smoking. Medical history, cardiovascular status, ECG, routine laboratory tests (such as haemoglobin, creatinine, amylase and liver values), blood pressure measurements and a 2-h oral glucose tolerance test were performed during the screening visit. Since this was a pioneer study on the effects of secretin on human BAT, we conducted three separate PET/CT scans with two different tracers. Thus, the cumulative radiation dose was 10.67 mSv and Ethics Committee approval was only applied for male participants. Written informed consent was provided by all participants.

PET/CT studies. Three metabolic PET/CT studies (GE Discovery™ ST System, General Electric Systems) of the neck were conducted according to the same

protocol after overnight fasting; once during controlled cold exposure[33], and twice at room temperature conditions during randomized intravenous secretin (secretin pentahydrochloride 1 IU kg⁻¹ × 2, Secrelux, Sanochemia) or placebo (saline) infusions.

First, a computed tomography scan of the neck was performed for attenuation correction, anatomic localization and the analysis of BAT radiodensity. A 1-min intravenous infusion of placebo or secretin was then administered, after which 500 MBq of [¹⁵O]H₂O was injected for measuring tissue perfusion[34]. A dynamic 6-min scan of the neck region was acquired, using the frames 6 × 5, 6 × 15 and 8 × 30 s. After radioactive decay, 150 MBq of [¹⁸F]FDG was administered for measuring GU[34] and a second 2-min infusion of placebo or secretin was initiated. Dynamic 40-min scanning was started simultaneously on the neck region (frames

$1 \times 1\,min$, $6 \times 30\,s$, $1 \times 1\,min$, $3 \times 5\,min$ and $2 \times 10\,min$). Arterialized venous plasma radioactivity samples were collected during the scan. Two hours after the first secretin infusion, another computed tomography scan of the neck was acquired for the analysis of BAT radiodensity. Radiotracers were produced at the Turku PET Centre.

PET/CT analysis. Image analysis was conducted with Carimas v.2.8 software (Turku PET Centre). Regions of interest (ROI) were manually outlined in the fusion images, composed of the dynamic [^{18}F]FDG PET image and the computed tomography image. To analyse BAT, ROI were drawn on the supraclavicular fat depots including only voxels with computed tomography HU within the adipose tissue range (-50 to $-250\,HU$)[22]. Skeletal muscle ROI were drawn on the deltoid muscles.

For tissue GU calculations, time activity curves (TAC) were generated for the ROI. Regional TAC data was analysed by taking into account the radioactivity in arterialized plasma using the Patlak model[35]. A lumped constant value of 1.14 was used for adipose tissue[36] and 1.20 for skeletal muscle[37].

To analyse the radiowater images, arterial input function was determined by drawing a ROI in the arch of aorta. The same BAT ROI from the FDG images were used for the analysis of BAT perfusion. Perfusion was calculated using the one-tissue compartment model as previously described[33].

To measure the change in radiodensity, again the same BAT ROI were used. The HU of BAT were compared between the first computed tomography scan of the neck (before administration of placebo or secretin), and the later computed tomography scan of the neck (at approximately 2 h after saline or secretin infusion)[22].

PET/CT images were analysed by S.L., who conducted the trial together with M.L and could thus not be fully blinded to the intervention. Half of the study participants' images were also analysed by M.U-D. to check the reproducibility of results. M.U-D. was blinded to the intervention.

Indirect calorimetry. Whole body energy expenditure was assessed with indirect calorimetry during each PET/CT scan (Deltatrac II, Datex-Ohmeda)[33]. The first minutes of calorimetry data were excluded to measure the steady state, and analysis started from 10 min after the first secretin dose. Whole body energy expenditure and the rate at which carbohydrates, lipids and protein was used for energy expenditure, were calculated using the Weir equation[38], as well as with the manufacturer's equations[39] with MATLAB (v.R2011a). Protein metabolism was calculated by assuming urine nitrogen as 13 g per 24 h. This analysis was done by M.U-D., who was blinded to the intervention.

fMRI studies. fMRI studies of the brain were conducted twice with an identical protocol, after overnight fasting. As in the metabolic PET/CT studies, secretin and placebo were administered at room temperature in a randomized order and participants were blinded to the intervention. fMRI food tasks were timed to correspond with the timing of the [^{18}F]FDG PET/CT scan of the neck region. We used a previously established task protocol[16] for inducing anticipatory reward, by showing the participants pictures of palatable (for example, chocolate, pizza, cakes) and bland (for example, lentils, cereal, eggs) food pictures. This task simulates situations where appetite is triggered by anticipating the actual feeding via visual food cues, such as those in advertisements. The pictures were rated in a previous study by independent participants; the ratings showed that the appetizing foods were evaluated more pleasant than the bland foods, $t(31) = 4.67$, $P < 0.001$ (ref. [40]). During the tasks, functional data were acquired with gradient echo-planar imaging (EPI) sequence, sensitive to the blood-oxygen level-dependent imaging (BOLD) signal.

Participants viewed alternating 16.2-s epochs with pictures of palatable or non-palatable foods. Each epoch contained nine stimuli from one category, intermixed with fixation crosses. Each food stimulus was presented on either the right or the left side of the screen, and participants were instructed to indicate its location by pressing corresponding buttons. This task was used simply to ensure that participants had to pay attention to the stimuli. Stimulus delivery was controlled by the Presentation software (Neurobehavioral System, Inc.). Functional data were acquired using 3-Tesla Philips Ingenuity PET/MR scanner and using EPI sequence with the following parameters: TR, 2,600 ms; TE, 30 ms; flip angle 75°, $240 \times 240 \times 135\,mm^3$ FOV, $3 \times 3 \times 3\,mm^3$ voxel size. Each volume consisted of 45 interleaved axial slices acquired in ascending order. A total of 165 functional volumes were acquired, with additional five dummy volumes acquired and discarded at the beginning of each run. Anatomical reference images were acquired using a T1-weighted sequence with following parameters: TR 8.1 ms, TE 3.7 ms, flip angle 7°, $256 \times 56 \times 176\,mm^3$ FOV, $1 \times 1 \times 1\,mm^3$ voxel size.

fMRI analysis. Preprocessing of MRI images was performed using FMRIPREP (v.1.3.0.2)[41], a Nipype (v.1.1.9)[42] based tool. Each T1-weighted image was corrected for intensity non-uniformity with N4BiasFieldCorrection (v.2.1.0)[43] and skull-stripped on the basis of the OASIS template with antsBrainExtraction. sh workflow (ANTs v.2.2.0). Brain surfaces were reconstructed using recon-all from FreeSurfer (v.6.0.0)[44], and the brain mask estimated previously was refined with a custom variation of the method to reconcile ANTs- and FreeSurfer-derived segmentations of the cortical grey matter using Mindboggle[45]. Spatial normalization to the ICBM 152 non-linear asymmetrical template v.2009c (ref. [46])

was done with non-linear registration using the antsRegistration tool[47]. Tissue segmentation of cerebrospinal fluid, white matter and grey matter was performed on the brain-extracted T1w using fast[48] from FSL (v.5.0.9).

Functional MRI images were slice time corrected with 3dTshift from AFNI (v.16.2.07)[49] and motion corrected with mcflirt[50] from FSL. This was followed by coregistration to the corresponding T1w via boundary-based registration[51] with nine degrees of freedom, using bbregister from FreeSurfer. There steps were concatenated and applied in a single step via antsApplyTransforms with the Lanczos interpolation. Physiological noise regressors were obtained using CompCor[52], where principal components were estimated for temporal and anatomical variants. A mask to exclude signal with cortical origin was created via eroding the brain mask, ensuring it merely originating from subcortical structures. Six temporal CompCor components were then calculated including the top 5% variable voxels within that subcortical mask. For anatomical CompCor components, six components were calculated within the intersection of the subcortical mask and the union of cerebral spinal fluid and white matter masks, after projection to the native space of each functional run. Frame-wise displacement[53] was calculated for each functional run using the implementation of Nipype. Finally, ICA-based automatic removal of motion artefacts was used to generate aggressive noise regressors and also to create a variant of data that is non-aggressively denoised[54].

The quality of images was assessed using fmriprep's visual reports, where data were manually inspected for whole-brain field of view coverage, alignment to the anatomical images and artefacts. Three participants in one of the two scans had large movement artefacts with more than 25% of the volumes exceeding 0.2-mm framewise displacement, and therefore a separate analysis excluding these participants ($n = 11$) was also performed (Fig. 3b).

CSS. We assessed satiety during the study days by measuring CSS. We used a validated VAS questionnaire[17,55] to calculate CSS (CSS = satiety + fullness + (100 − prospective food consumption) + (100 − hunger)) (Extended Data Fig. 2). All questions were answered in Finnish. Participants filled in the questionnaire in three different phases of the study: preprandial (at baseline and after the scan), prandial (10 min into feeding) and postprandial (directly after feeding, then every 30 min up to 2 h after feeding).

Dietary intake. Participants were instructed to eat and live normally before and after the scanning days, avoiding heavy exertion and events that involve excessive feeding or alcohol consumption. The participants were also instructed to pay attention to eating similar foods at similar time points the day before both scans. Fasting was instructed to begin at 22:00 the previous night and continued until the scan. All scans were conducted between 8:00 and 11:00. and each paired scan was booked for the same timeslot, to control for the effect of time on hunger.

After the fMRI scan, participants were offered a standardized meal (1 kg of pasta and minced-meat casserole, Supplementary Table 4) and advised to eat at their own pace until they felt satiated. Participants ate at the PET Centre kitchen without outside disturbances for 20 min. They filled in a VAS questionnaire and the food container was weighed at 10 and 20 min after the start of meal, to assess whether secretin has an effect on the size of the first meal after an overnight fast.

Dietary intake of energy and energy yielding nutrients were calculated from 6-d food diaries, recorded by the participants as follows: 2 d before fMRI scan, on the day of scanning and 3 d after scanning (for the results, see Supplementary Table 1). These days included both weekends and weekdays. These data were acquired to check for compliance with the protocol, as well as assessing the effect of preprandially administered secretin on dietary intake. The participants were given instructions on how to record their food intake during screening visits. Diaries were checked for completeness and accuracy with the help of an illustrated portion booklet at the end of the study. The mean daily intake of energy and nutrients was calculated by using computerized software (Aivo diet v.2.0.2.3, Aivo). Two participants were excluded from analysis due to protocol deviations in reporting.

Serum and plasma samples. Samples were collected from the antecubital vein through a cannula during PET/CT scans. Serum samples were collected at baseline, and after 10, 20, 30, 60 and 120 min. Plasma samples were collected at baseline, 20, 30, 60 and 120 min. We also collected serum samples for bile acid analysis during fMRI scans at 0, 15 and 50 min. The fewer time points were used because samples cannot be collected during the on-going MRI sequences. Serum samples were analysed for metabolites (such as serum NEFAs) at the Nightingale laboratory with nuclear magnetic resonance spectroscopy[56]. Plasma samples for glucose, insulin, TSH, free T4 and free T3 were analysed with electrochemiluminescence immunoassays at the Turku University Hospital laboratory. Serum samples for bile acids were analysed at the VITA laboratory with an accredited photometric, kinetic method. Serum secretin were determined by enzyme-linked immunosorbent assay using a kit purchased from Cloud-Clone, following the manufacturer's instructions. Secretin concentrations were calculated using a standard curve generated by secretin standards included in the kit.

BAT biopsies and immunohistochemistry analysis. Biopsies were obtained in non-fasting state on a separate, late afternoon visit ($n = 6$). BAT samples were

collected in local anaesthesia from a single incision by an experienced plastic surgeon (T.N.), under the supervision of an anaesthesiologist (M.T.). Samples were preserved in formalin. Immunohistochemistry was performed on formalin-fixed paraffin embedded tissue specimen, using a Bond RXm system (Leica, all reagents from Leica) with a primary rabbit polyclonal antibody against SCTR (HPA007269, Sigma-Aldrich; diluted 1:200 in antibody diluent). Briefly, slides were deparaffinized using deparaffinization solution, pretreated with Epitope retrieval solution 2 (corresponding to EDTA buffer pH 9) for 30 min. Antibody binding was detected with a polymer refine detection kit without post primary reagent and visualized with 3,3′-diaminobenzidine as a dark brown precipitate. Counterstaining was done with haematoxyline. As a technical negative control, consecutive slides were stained without primary antibody. All slides were scanned using a high-throughput slide scanning system (AT2, Leica), evaluated by an experienced comparative pathologist (K.S.) and representative images were taken using the Imagescope software (v.12.4.0.7018, Leica).

Regulation of *SCTR* gene expression in BAT. To further expand on the regulation of *SCTR* in BAT, we investigated *SCTR* gene expression in two additional cohorts, as well as in murine interscapular BAT and primary murine brown adipocytes differentiated in cell culture. We analysed the *SCTR* mRNA level in BAT biopsies from fasted (*n* = 14) and non-fasted (*n* = 14) healthy men recruited in previous studies[9,18]. For proof of concept, gene expression on the mRNA level was also analysed from fasted versus ad libitum fed mice, as well as primary BAT cell cultures, stimulated with varying concentrations of secretin.

Non-fasted and fasted human BAT biopsies. Non-fasted (*n* = 14, mean (s.d.), age 37.8 (10.4) years, BMI 26.1 (4.7) kg m^{-2}) supraclavicular BAT samples were analysed from a previously reported study[9]. Supraclavicular BAT was localized from cold exposure scans and samples were collected at room temperature in local anaesthesia from a single incision by a plastic surgeon (T.N.), as described previously[9]. Samples were frozen in liquid nitrogen. The study protocol was reviewed and approved by the Ethics Committee of the Hospital District of Southwest Finland.

Fasted (*n* = 14, mean (s.d.), age 23.4 (3.6) years, BMI 23.0 (1.9) kg m^{-2}) supraclavicular BAT biopsy samples were provided from a clinical study registered under the ClinicalTrials.gov identifier no. NCT03189511. The location of metabolically active brown fat in the supraclavicular region was determined by [^{18}F]FDG PET/MR as described previously[18]. The volunteer arrived in a fasted state and biopsies were collected with an ultrasound-guided coaxial core-needle (16G size, 10 mm core length, BARD Mission) under local anaesthesia. Samples were immediately cleaned from blood and connective tissue, and frozen in liquid nitrogen. The study was approved by the ethics committee of the canton of Zurich.

Animal experiments and primary brown adipocytes. Animal experiments were approved by the German animal welfare authorities at the district government (approval no. 55.2-1-54-2532-34-2016). Mice were bred at the specific-pathogen free animal facility of Technical University of Munich. They had ad libitum access to food and water and were maintained at 22 s.d., 1 °C and 50–60% relative humidity in a 12 h:12 h light:dark cycle. Male 129S6/SvEV mice were used for the fasting experiment. Food was removed for 18 h including one dark phase. Subsequent to fasting and ad libitum feeding mice were killed in the morning and BAT was collected and snap-frozen.

For primary cell culture BAT was obtained from 5-week-old 129S6/SvEV mice. For each experiment tissue from two mice was pooled and digested with collagenase, as described previously[57]. Stromal vascular fraction cells were seeded, grown to confluency and differentiated into mature adipocytes, following a standard protocol. Adipocyte differentiation was induced for 48 h with 5 µg ml^{-1} insulin, 1 nM 3,3′,5-triiodo-l-thyronine (T3), 125 µM indomethacin, 500 µM isobutylmethylxanthine and 1 µM dexamethasone in adipocyte culture media (DMEM supplemented with 10% heat-inactivated foetal bovine serum, penicillin/streptomycin). Cells were then maintained in adipocyte culture media supplemented with 5 µg ml^{-1} insulin and 1 nM T3 for 6 d with media change every 2 d. Before collection on day 7 of differentiation, mature primary brown adipocytes were stimulated with varying concentrations of secretin (Tocris, catalogue no. 1919) for 12 h.

RNA extraction and gene expression analysis. For human BAT samples, total RNA was extracted from tissues using Trizol reagent (Invitrogen) according to the manufacturer's instructions. DNase treatment (NEB BioLabs) was included to remove traces of genomic DNA. Reverse transcription was performed to generate a complementary DNA library by using the High Capacity cDNA Reverse transcription kit (Applied Biosystems). Quantitative PCR (qPCR) was performed on ViiA7 instrument (Applied Biosystems) using Fast SYBR Green Master Mix (Applied Biosystems). Relative mRNA concentrations of *SCTR* (forward: AAAGTACCTCCAGGGATTTGTG, reverse: CAATAGCCCACAAAGCAACA) normalized to the expression of *RPL13A1* (forward: GGACCGTGCGAGGTATGCT, reverse: ATGCCGTCAAACACCTTGAGA) were calculated by the ΔC_t method.

From mouse BAT and primary brown adipocytes, total RNA was isolated using Trisure (Bioline) and purified using the SV total RNA Isolation System (Promega) from cultured cells or frozen tissue samples (129S6/SvEV). Reverse transcriptase reactions were performed using SensiFAST cDNA Synthesis Kit (Bioline). Real-time qPCR was performed with SYBR green fluorescent dye in 384-well format using LightCycler 480 (Roche). General transcription Factor IIB (Gtf2b) served as an internal control. To be able to calculate relative gene expression levels of samples, standard reactions containing serial diluted pooled cDNA of all samples (Pure, 1:2, 1:4, 1:8, 1:16, 1:32 and 1:64) as a template were used to establish a standard curve. The RNA abundance of *Ucp1* gene was normalized to the housekeeping gene *Gtf2b*. The following primers were used:

Sctr F: 5′-ATGCACCTGTTTGTGTCCTT-3′ R: 5′-TAGTTGGCCATGATGCAGTA-3′

Gtf2b F: 5′-TGGAGATTTGTCCACCATGA-3′ R: 5′-GAATTGCCAAACTCATCAAAACT-3′

Statistical analysis. Sample size (*n* = 14) was determined by power calculations based on the BAT GU of participants (*n* = 6) reported in our previous study[12]. Sample size calculation was performed with power 0.8, significance level 0.05 and effect size 0.900 with G*power for Wilcoxon's signed-rank matched pairs test. An *n* = 15 was decided as the final sample size, To account for possible loss of data. The primary outcome measure of the first part of the study was BAT activity, while whole body energy expenditure was listed as a secondary outcome measure. For the second part of the study, brain BOLD activity during palatable versus non-palatable food image fMRI scans, was listed as the primary outcome measure, while CSS and calorie intake were secondary outcome measures.

Data are reported as means and s.d. when differences between paired observations are normally distributed, and otherwise as median and IQR. BAT activity is expressed as GU (µmol 100 g min^{-1}) and perfusion (ml per 100 g per min). BAT radiodensity is expressed in HU. Whole body energy expenditure, carbohydrate oxidation and fat oxidation by indirect calorimetry measurements are expressed in kcal d^{-1}. Whole body oxygen consumption by indirect calorimetry measurement is expressed in ml min^{-1}. Dietary intake is expressed in kcal.

All tests used were two-sided. A paired samples *t*-test was used when differences between paired observations were normally distributed (BAT perfusion, muscle GU, calorimetry, CSS, AUC and food diary data), and a Wilcoxon signed-rank test was used otherwise (BAT GU). An unpaired *t*-test was used for murine mRNA data. For effect size, Cohen's *d* was calculated for the paired *t*-test and *r* for the Wilcoxon signed-rank test[58]. Correlations were analysed with Pearson's correlation for linear and Spearman's rank correlation for non-linear associations between paired observations. Statistical analysis for PET/CT, calorimetry and food diary data was performed with IBM SPSS Statistics (v.25 and 27).

Functional MRI data was analysed using SPM12 (v.7487) run with MATLAB (v.R2016b). In the analysis, the whole-brain random effects model was applied using a two-stage process with separate first and second levels. For each participant, the general linear model was first used to predict regional effects of task parameters (palatable and non-palatable foods) and drug condition (secretin, placebo) on BOLD indices of activation. Participant-wise contrast images were generated for the effect of palatable versus non-palatable foods in the secretin and placebo conditions, as well as an interaction effect between food categories and conditions, and subjected to second-level analyses. The resulting statistical images were thresholded at *P* < 0.05, false discovery rate corrected[59].

For serum metabolites and biomarkers, plasma hormones and CSS, we carried out statistical analysis using R v.3.6.0 (2019-04-26), with R packages: readxl v.1.3.1, pheatmap v.1.0.12 and gdata v.2.18.0. Preprandial, prandial and postprandial phase CSS analysis was carried out using GraphPad Prism8. In repeated measures, values for each exercise (placebo or secretin intervention for a participant) were normalized by dividing by the value of the first time point. Placebo and secretin interventions were compared using a paired Wilcoxon signed-rank test for each time point and AUC. Spearman's rank correlation and *P* value were calculated for the GU (muscle GU and BAT GU values) and normalized pancreas related hormones (secretin and insulin) at each time point up to 60 min. Non-parametric tests were used to avoid assumptions around linearity of associations.

Randomized allocation sequences for the order of placebo and secretin interventions were generated with the randomized blocks method, with a block size of six, using SAS (v.9.4 for Windows). The allocation sequence was generated by the Turku University statistics department, which was not otherwise involved in the study. Participants were assigned to the sequence in order of enrolment by study personnel enrolling participants into the study.

Reporting Summary. Further information on research design is available in the Nature Research Reporting Summary linked to this article.

Data availability

All statistical parametric images of the fMRI study (including the effect size maps) can be found from NeuroVault at https://neurovault.org/collections/ECURNRON/. The accession number for the RNA-Seq data presented in this article is GEO GSE113764. *SCTR* expression in human tissues is available in the Online Biology

Gene Portal System (BioGPS) at http://ds.biogps.org/?dataset=GSE1133&gene=6344. Datasets that support the findings of this study are available in the Supplementary Information. Source data are provided with this paper. The data that support the plots within this paper, as well as other findings of this study, are available from the corresponding author (P.N.) upon reasonable request.

References

1. Virtanen, K. A. et al. Functional brown adipose tissue in healthy adults. *N. Engl. J. Med.* **360**, 1518–1525 (2009).
2. Cypess, A. M. et al. Identification and importance of brown adipose tissue in adult humans. *N. Engl. J. Med.* **360**, 1509–1517 (2009).
3. van Marken Lichtenbelt, W. D. et al. Cold-activated brown adipose tissue in healthy men. *N. Engl. J. Med.* **360**, 1500–1508 (2009).
4. Blondin, D. P. et al. Contributions of white and brown adipose tissues and skeletal muscles to acute cold-induced metabolic responses in healthy men. *J. Physiol.* **593**, 701–714 (2015).
5. Villarroya, F., Cereijo, R., Villarroya, J. & Giralt, M. Brown adipose tissue as a secretory organ. *Nat. Rev. Endocrinol.* **13**, 26–35 (2017).
6. Kajimura, S., Spiegelman, B. M. & Seale, P. Brown and beige fat: physiological roles beyond heat generation. *Cell Metab.* **22**, 546–559 (2015).
7. Rothwell, N. J. & Stock, M. J. A role for brown adipose tissue in diet-induced thermogenesis. *Nature* **281**, 31–35 (1979).
8. Glick, Z., Teague, R. J. & Bray, G. A. Brown adipose tissue: thermic response increased by a single low protein, high carbohydrate meal. *Science* **213**, 1125–1127 (1981).
9. U Din, M. et al. Postprandial oxidative metabolism of human brown fat indicates thermogenesis. *Cell Metab.* **28**, 207–216.e3 (2018).
10. Chondronikola, M., Porter, C., Malagaris, I., Nella, A. A. & Sidossis, L. S. Brown adipose tissue is associated with systemic concentrations of peptides secreted from the gastrointestinal system and involved in appetite regulation. *Eur. J. Endocrinol.* **177**, 33–40 (2017).
11. Crovetti, R., Porrini, M., Santangelo, A. & Testolin, G. The influence of thermic effect of food on satiety. *Eur. J. Clin. Nutr.* **52**, 482–488 (1998).
12. Li, Y. et al. Secretin-activated brown fat mediates prandial thermogenesis to induce satiation. *Cell* **175**, 1561–1574.e12 (2018).
13. Blondin, D. et al. Inhibition of intracellular triglyceride lipolysis suppresses cold-induced BAT metabolism and increases shivering in humans. *Cell Metab.* **25**, 438–447 (2017).
14. Wu, C., Jin, X., Tsueng, G., Afrasiabi, C. & Su, A. I. BioGPS: building your own mash-up of gene annotations and expression profiles. *Nucleic Acids Res.* **44**, D313–D316 (2016).
15. Su, A. I. et al. A gene atlas of the mouse and human protein-encoding transcriptomes. *Proc. Natl Acad. Sci. USA.* **101**, 6062–6067 (2004).
16. Nummenmaa, L. et al. μ-opioid receptor system mediates reward processing in humans. *Nat. Commun.* **9**, 1500 (2018).
17. Gilbert, J.-A. et al. The effect of tesofensine on appetite sensations. *Obesity* **20**, 553–561 (2012).
18. Balaz, M. et al. Inhibition of mevalonate pathway prevents adipocyte browning in mice and men by affecting protein prenylation. *Cell Metab.* **29**, 901–916.e8 (2019).
19. Sekar, R. & Chow, B. K. C. Lipolytic actions of secretin in mouse adipocytes. *J. Lipid Res.* **55**, 190–200 (2014).
20. Butcher, R. W. & Carlson, L. A. Effects of secretin on fat mobilizing lipolysis and cyclic AMP levels in rat adipose tissue. *Acta Physiol. Scand.* **79**, 559–563 (1970).
21. Raiko, J. et al. Brown adipose tissue triglyceride content is associated with decreased insulin sensitivity, independently of age and obesity. *Diabetes, Obes. Metab.* **17**, 516–519 (2015).
22. U Din, M. et al. Human brown fat radiodensity indicates underlying tissue composition and systemic metabolic health. *J. Clin. Endocrinol. Metab.* **102**, 2258–2267 (2017).
23. Yaney, G. C. & Corkey, B. E. Fatty acid metabolism and insulin secretion in pancreatic beta cells. *Diabetologia* **46**, 1297–1312 (2003).
24. Stein, D. T. et al. The insulinotropic potency of fatty acids is influenced profoundly by their chain length and degree of saturation. *J. Clin. Invest.* **100**, 398–403 (1997).
25. Afroze, S. et al. The physiological roles of secretin and its receptor. *Ann. Transl. Med.* **1**, 29 (2013).
26. Broeders, E. P. M. et al. The bile acid chenodeoxycholic acid increases human brown adipose tissue activity. *Cell Metab.* **22**, 418–426 (2015).
27. Amin, A., Dhillo, W. S. & Murphy, K. G. The central effects of thyroid hormones on appetite. *J. Thyroid Res.* **2011**, 306510 (2011).
28. Bianco, A. C. & Silva, J. E. Intracellular conversion of thyroxine to triiodothyronine is required for the optimal thermogenic function of brown adipose tissue. *J. Clin. Invest.* **79**, 295–300 (1987).
29. Lahesmaa, M. et al. Hyperthyroidism increases brown fat metabolism in humans. *J. Clin. Endocrinol. Metab.* **99**, E28–E35 (2014).
30. Bessesen, D. H. & Van Gaal, L. F. Progress and challenges in anti-obesity pharmacotherapy. *Lancet Diabetes Endocrinol.* **6**, 237–248 (2018).
31. van Ooijen, A. M. J., van Marken Lichtenbelt, W. D., van Steenhoven, A. A. & Westerterp, K. R. Seasonal changes in metabolic and temperature responses to cold air in humans. *Physiol. Behav.* **82**, 545–553 (2004).
32. Yoneshiro, T. et al. Recruited brown adipose tissue as an antiobesity agent in humans. *J. Clin. Invest.* **123**, 3404–3408 (2013).
33. U.-Din, M. et al. Human brown adipose tissue [15O]O₂ PET imaging in the presence and absence of cold stimulus. *Eur. J. Nucl. Med. Mol. Imag.* https://doi.org/10.1007/s00259-016-3364-y (2016).
34. Orava, J. et al. Different metabolic responses of human brown adipose tissue to activation by cold and insulin. *Cell Metab.* **14**, 272–279 (2011).
35. Patlak, C. S. & Blasberg, R. G. Graphical evaluation of blood-to-brain transfer constants from multiple-time uptake data. Generalizations. *J. Cereb. Blood Flow. Metab.* **5**, 584–590 (1985).
36. Virtanen, K. A. et al. Human adipose tissue glucose uptake determined using [18 F]-fluoro-deoxy-glucose ([18 F]FDG) and PET in combination with microdialysis. *Diabetologia* **44**, 2171–2179 (2001).
37. Peltoniemi, P. et al. Lumped constant for [18 F]fluorodeoxyglucose in skeletal muscles of obese and nonobese humans. *Am. J. Physiol. Metab.* **279**, E1122–E1130 (2000).
38. Weir, J. B. & de, V. New methods for calculating metabolic rate with special reference to protein metabolism. *J. Physiol.* **109**, 1–9 (1949).
39. Meriläinen, P. T. Metabolic monitor. *Int. J. Clin. Monit. Comput.* **4**, 167–177 (1987).
40. Nummenmaa, L. et al. Dorsal striatum and its limbic connectivity mediate abnormal anticipatory reward processing in obesity. *PLoS ONE* **7**, e31089 (2012).
41. Esteban, O. et al. fMRIPrep: a robust preprocessing pipeline for functional MRI. *Nat. Methods* https://doi.org/10.1038/s41592-018-0235-4 (2019).
42. Gorgolewski, K. et al. Nipype: A flexible, lightweight and extensible neuroimaging data processing framework in Python. *Front. Neuroinform.* https://doi.org/10.3389/fninf.2011.00013 (2011).
43. Tustison, N. J. et al. N4ITK: Improved N3 bias correction. *IEEE Trans. Med. Imag.* https://doi.org/10.1109/TMI.2010.2046908 (2010).
44. Dale, A. M., Fischl, B. & Sereno, M. I. Cortical surface-based analysis: I. Segmentation and surface reconstruction. *Neuroimage* https://doi.org/10.1006/nimg.1998.0395 (1999).
45. Klein, A. et al. Mindboggling morphometry of human brains. *PLoS Comput. Biol.* https://doi.org/10.1371/journal.pcbi.1005350 (2017).
46. Fonov, V., Evans, A., McKinstry, R., Almli, C. & Collins, D. Unbiased nonlinear average age-appropriate brain templates from birth to adulthood. *Neuroimage* https://doi.org/10.1016/s1053-8119(09)70884-5 (2009).
47. Avants, B. B., Epstein, C. L., Grossman, M. & Gee, J. C. Symmetric diffeomorphic image registration with cross-correlation: evaluating automated labeling of elderly and neurodegenerative brain. *Med. Image Anal.* https://doi.org/10.1016/j.media.2007.06.004 (2008).
48. Zhang, Y., Brady, M. & Smith, S. Segmentation of brain MR images through a hidden Markov random field model and the expectation-maximization algorithm. *IEEE Trans. Med. Imag.* https://doi.org/10.1109/42.906424 (2001).
49. Cox, R. W. AFNI: Software for analysis and visualization of functional magnetic resonance neuroimages. *Comput. Biomed. Res.* https://doi.org/10.1006/cbmr.1996.0014 (1996).
50. Jenkinson, M., Bannister, P., Brady, M. & Smith, S. Improved optimization for the robust and accurate linear registration and motion correction of brain images. *Neuroimage* https://doi.org/10.1016/S1053-8119(02)91132-8 (2002).
51. Greve, D. N. & Fischl, B. Accurate and robust brain image alignment using boundary-based registration. *Neuroimage* https://doi.org/10.1016/j.neuroimage.2009.06.060 (2009).
52. Behzadi, Y., Restom, K., Liau, J. & Liu, T. T. A component based noise correction method (CompCor) for BOLD and perfusion based fMRI. *Neuroimage* https://doi.org/10.1016/j.neuroimage.2007.04.042 (2007).
53. Power, J. D. et al. Methods to detect, characterize, and remove motion artifact in resting state fMRI. *Neuroimage* https://doi.org/10.1016/j.neuroimage.2013.08.048 (2014).
54. Pruim, R. H. R. et al. ICA-AROMA: a robust ICA-based strategy for removing motion artifacts from fMRI data. *Neuroimage* https://doi.org/10.1016/j.neuroimage.2015.02.064 (2015).
55. Flint, A., Raben, A., Blundell, J. E. & Astrup, A. Reproducibility, power and validity of visual analogue scales in assessment of appetite sensations in single test meal studies. *Int. J. Obes. Relat. Metab. Disord.* **24**, 38–48 (2000).
56. Soininen, P. et al. High-throughput serum NMR metabonomics for cost-effective holistic studies on systemic metabolism. *Analyst* **134**, 1781 (2009).
57. Li, Y., Fromme, T., Schweizer, S., Schöttl, T. & Klingenspor, M. Taking control over intracellular fatty acid levels is essential for the analysis of thermogenic function in cultured primary brown and brite/beige adipocytes. *EMBO Rep.* **15**, 1069–1076 (2014).

58. Rosenthal, R. in *The Handbook of Research Synthesis* (eds Cooper, H. et al.) 231–244 (Russell Sage Foundation, 1994).
59. Benjamini, Y. & Hochberg, Y. Controlling the false discovery rate—a practical and powerful approach to multiple testing. *J. R. Stat. Soc. Ser. B-Methodol.* **57**, 289–300 (1995).

Acknowledgements

Author contributions

M.K., P.N., K.A.V. and S.L. conceived and designed the study. S.L., L.S. and M.L. performed the human experiments. K. Schnabl conceived the study design for the SCTR expression and regulation study and carried out animal and cell culture experiments. S.L., L.S., K. Schnabl, K.L., M.U.-D. and R.K analysed data. L.N., L.L.E. and T.V. helped with statistical analysis. O.E. and A.K.K. contributed to PET/CT data collection. K. Steiger conducted the immunohistochemical studies. L.N. conceived the fMRI study design. T.N. and M.T. provided BAT biopsies from study participants. M.B. and C.W. provided the analysis of fasted human BAT biopsies. K. Schnabl, Y.L and M.K edited the paper and contributed physiological aspects of secretin-activated brown fat in mouse studies complementing the human study. S.L. wrote the paper with input from authors. All authors read and approved the paper.

Competing interests

M.K. and Y.L. are inventors on a patent application from the Technical University of Munich (publication no. WO/2017/20285; international application no. PCT/EP2017/062420) addressing the role of SCTR agonists and modulators in the regulation of energy homeostasis. This patent is based on the initial discovery that meal-induced secretin inhibits food intake, and this anorexigenic action of secretin depends on the activation of brown fat[12]. The remaining authors declare no competing interests.

Additional information

Extended data is available for this paper at https://doi.org/10.1038/s42255-021-00409-4.

Supplementary information The online version contains supplementary material available at https://doi.org/10.1038/s42255-021-00409-4.

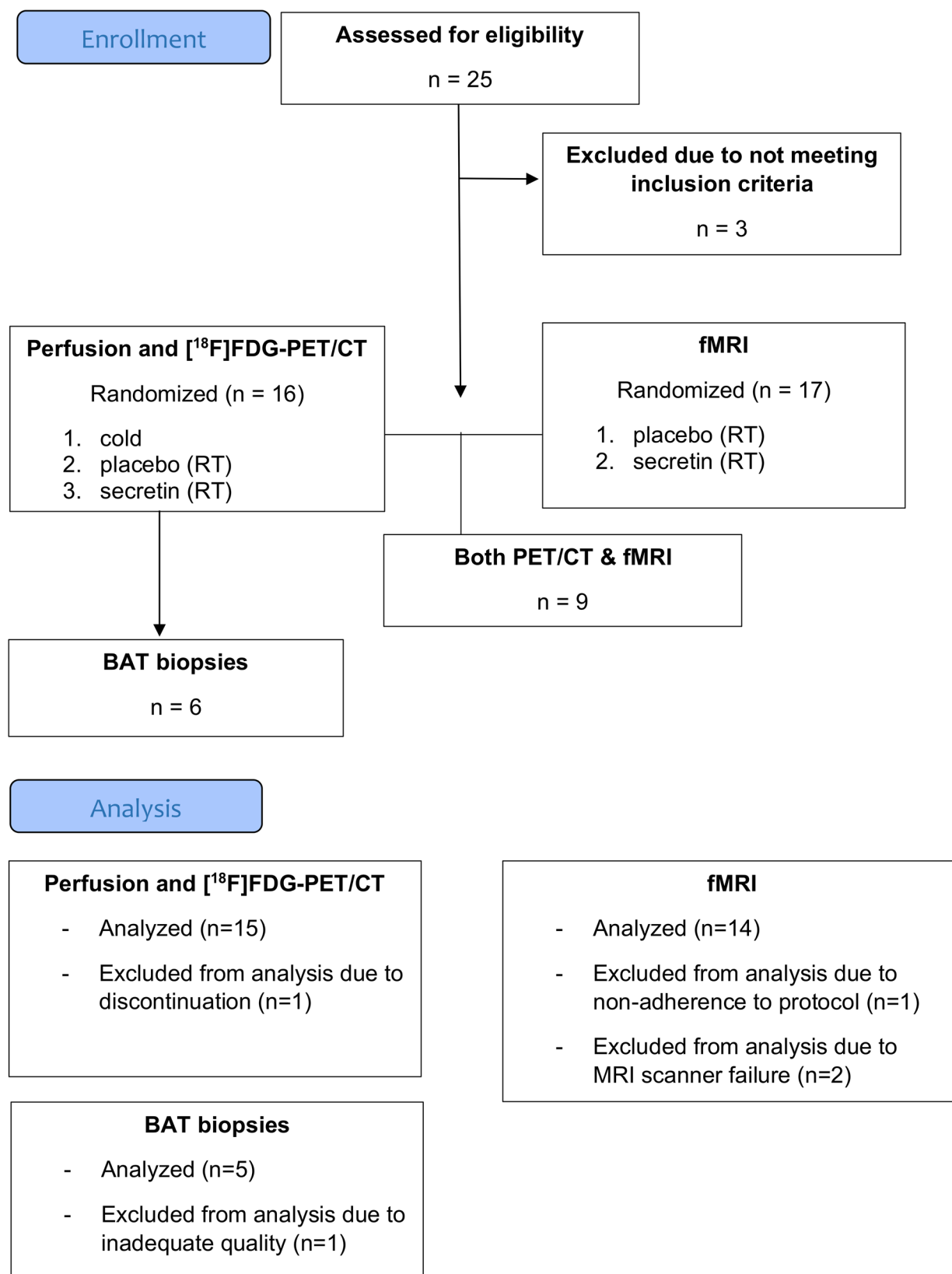**Correspondence and requests for materials** should be addressed to P.N.

Peer review information *Nature Metabolism* thanks Andrew Gray, Marc Tittgemeyer and the other, anonymous, reviewer(s) for their contribution to the peer review of this work. Primary Handling Editor: Christoph Schmitt.

Reprints and permissions information is available at www.nature.com/reprints.

Publisher's note Springer Nature remains neutral with regard to jurisdictional claims in published maps and institutional affiliations.

Enrollment

Assessed for eligibility

n = 25

Excluded due to not meeting inclusion criteria

n = 3

Perfusion and [^{18}F]FDG-PET/CT

Randomized (n = 16)

1. cold
2. placebo (RT)
3. secretin (RT)

fMRI

Randomized (n = 17)

1. placebo (RT)
2. secretin (RT)

Both PET/CT & fMRI

n = 9

BAT biopsies

n = 6

Analysis

Perfusion and [^{18}F]FDG-PET/CT

- Analyzed (n=15)

- Excluded from analysis due to discontinuation (n=1)

fMRI

- Analyzed (n=14)

- Excluded from analysis due to non-adherence to protocol (n=1)

- Excluded from analysis due to MRI scanner failure (n=2)

BAT biopsies

- Analyzed (n=5)

- Excluded from analysis due to inadequate quality (n=1)

Extended Data Fig. 1 | Enrolment and analysis. CONSORT flowchart on the enrolment and analysis of study participants.

How hungry do you feel?

I am not
hungry at all

I have never been
more hungry

How satisfied do you feel?

I am completely
empty

I cannot eat
another bite

How full do you feel?

Not at all full

Totally full

How much do you think you can eat?

Nothing at all

A lot

Extended Data Fig. 2 | Visual analogue scale –questions. Composite satiety score calculated with scale 1–100. Composite satiety score = satiety + fullness + (100 − prospective food consumption) + (100 − hunger)).
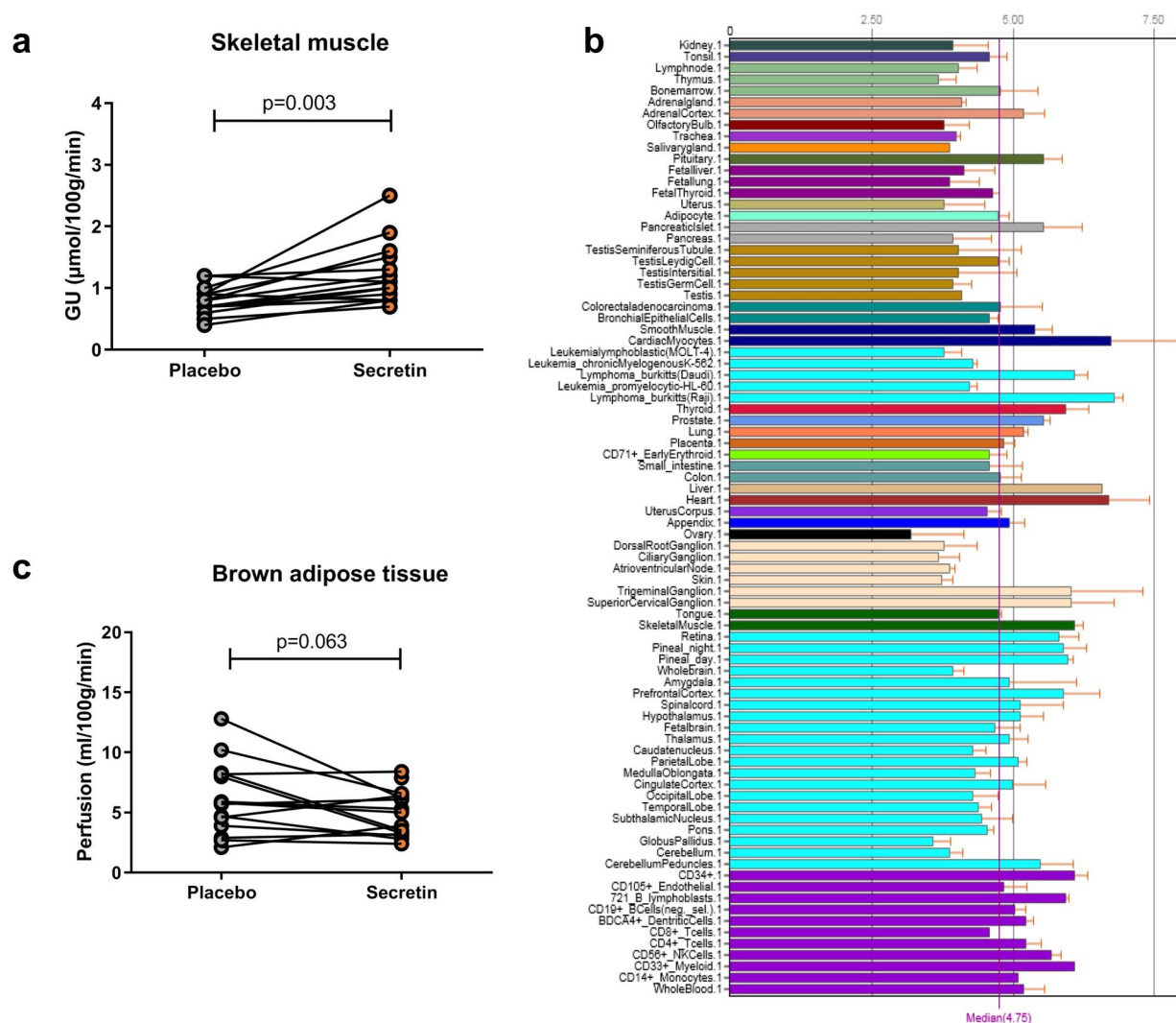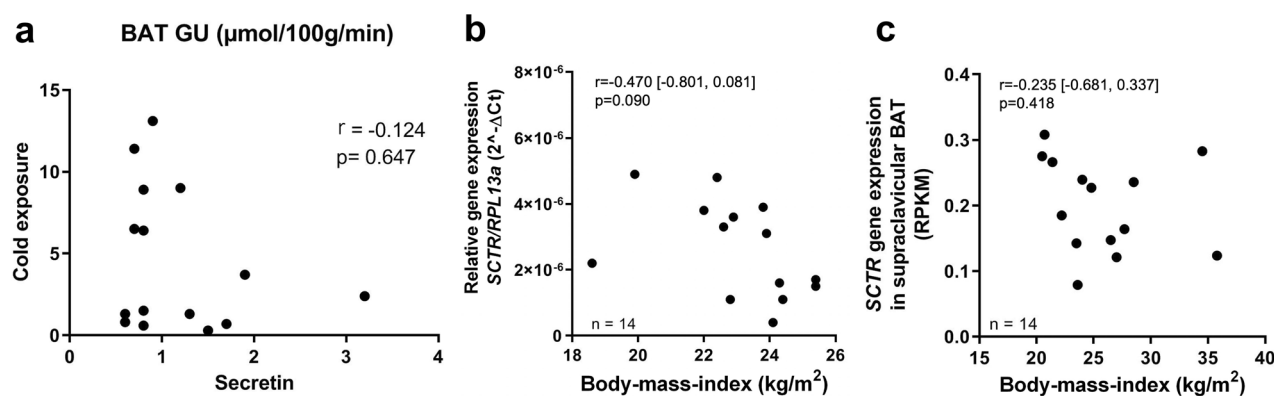
Extended Data Fig. 3 | PET results and secretin receptor expression. a. Muscle glucose uptake (GU) is increased by secretin compared to placebo. Data were analyzed with two-sided paired samples t-test and included n = 15 subjects. **b**. Secretin receptor expression in 79 human tissues, retrieved from http://ds.biogps.org/?dataset=GSE1133&gene=6344. Data are expressed as fold over the median (M), error bars show standard error. **c**. There is no significant change in perfusion after secretin infusion as compared to placebo. Data were analyzed with two-sided paired samples t-test and included n = 15 subjects.
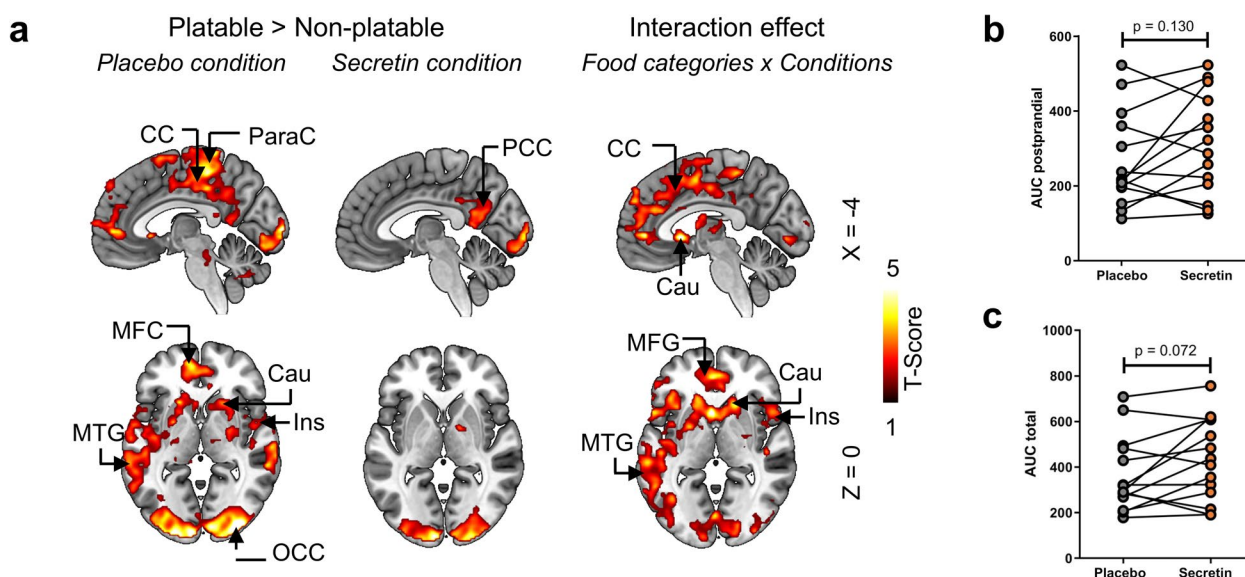
Extended Data Fig. 4 | Additional functional magnetic resonance and composite satiety score results. a, Down-regulated brain reward anticipation response due to injection of secretin. This separate analysis (n = 14) including subjects with high movement artifacts was originally done. In the placebo condition, palatable food led to increased BOLD activity in brain reward circuits. This effect was diminished in the secretin condition. Interaction effect between food categories and conditions were found in the reward circuits. Significance level was FDR-corrected at p value 0.05. MFC = medial frontal cortex, CC = cingulate cortex, OCC = occipital cortex, Cau = caudate, MTG = middle temporal gyrus, Ins = insula, PCC = posterior cingulate cortex. **b**, composite satiety score area under the curve (AUC) was not increased postprandially, c nor for the entire study day (pre-prandial, prandial and postprandial phases together). Values are normalized, dividing by the value of the first time point. Data were analyzed by two-sided paired samples t-test, n = 14.

Extended Data Fig. 5 | Additional positron emission tomography and secretin receptor gene expression results. a, Brown adipose tissue (BAT) glucose uptake (GU) in cold and after secretin. There is no correlation between BAT GU in cold exposure and after secretin infusion. Data were analyzed by Spearman's rank correlation in order to avoid assumptions around linearity of associations (n = 15). **b**, human secretin receptor (SCTR) expression on mRNA level, assessed by qPCR, in supraclavicular BAT is weakly associated with body-mass-index (BMI) in n = 14 fasted participants. Data were analyzed by Pearson's correlation. **c**, SCTR expression analyzed by RNASeq does not correlate with BMI in n = 14 non-fasted participants. Data were analyzed by Pearson's correlation.
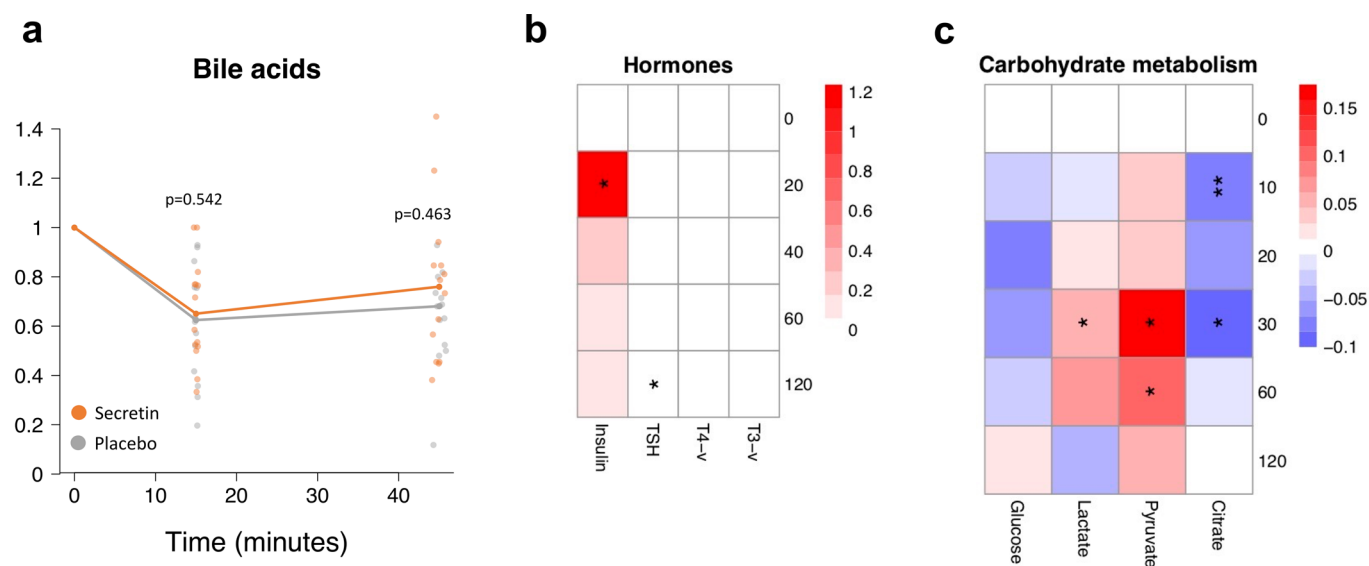
Extended Data Fig. 6 | Changes in circulating bile acids, hormones and carbohydrates. a. Secretin did not increase serum bile acid levels compared to placebo. Values are normalized, dividing by the value of the first time point. Each timepoint was analyzed by two-sided, paired Wilcoxon signed-rank test. Median values and standard errors are shown on graph, n = 14. **b**. Serum hormone and c. carbohydrate heatmap secretin vs. placebo. Values are normalized, dividing by the value of the first time point. Each timepoint was analyzed by two-sided paired Wilcoxon signed-rank test, n = 12. * = p < 0.05, ** = p < 0.01, *** p < 0.001.

Corresponding author(s):   Pirjo Nuutila

Last updated by author(s): 12.4.2021

Reporting Summary

Nature Research wishes to improve the reproducibility of the work that we publish. This form provides structure for consistency and transparency in reporting. For further information on Nature Research policies, see our Editorial Policies and the Editorial Policy Checklist.

Statistics

For all statistical analyses, confirm that the following items are present in the figure legend, table legend, main text, or Methods section.

n/a	Confirmed	
☐	☒	The exact sample size (*n*) for each experimental group/condition, given as a discrete number and unit of measurement
☐	☒	A statement on whether measurements were taken from distinct samples or whether the same sample was measured repeatedly
☐	☒	The statistical test(s) used AND whether they are one- or two-sided *Only common tests should be described solely by name; describe more complex techniques in the Methods section.*
☐	☒	A description of all covariates tested
☐	☒	A description of any assumptions or corrections, such as tests of normality and adjustment for multiple comparisons
☐	☒	A full description of the statistical parameters including central tendency (e.g. means) or other basic estimates (e.g. regression coefficient) AND variation (e.g. standard deviation) or associated estimates of uncertainty (e.g. confidence intervals)
☐	☒	For null hypothesis testing, the test statistic (e.g. F, t, r) with confidence intervals, effect sizes, degrees of freedom and P value noted *Give P values as exact values whenever suitable.*
☒	☐	For Bayesian analysis, information on the choice of priors and Markov chain Monte Carlo settings
☐	☒	For hierarchical and complex designs, identification of the appropriate level for tests and full reporting of outcomes
☐	☒	Estimates of effect sizes (e.g. Cohen's *d*, Pearson's *r*), indicating how they were calculated

Our web collection on statistics for biologists contains articles on many of the points above.

Software and code

Policy information about availability of computer code

Data collection	PET-CT image: Carimas 2.8 software https://turkupetcentre.fi/carimas/ fMRI: Presentation software (Neurobehavioral System, Inc., Berkeley, CA, USA) Daily intake of energy and nutrients: Aivo diet 2.0.2.3;Aivo
Data analysis	IBM SPSS Statistics (version 25 and 27), Matlab (version R2016b), SPM12 (version7487), FMRIPREP (version 1.3.0.2), Nipype (version 1.1.9), N4BiasFieldCorrection (version 2.1.0), OASIS template with antsBrainExtraction.sh workflow (ANTs version 2.2.0), FreeSurfer (version 6.0.0), the ICBM 152 Nonlinear Asymmetrical template version 2009c and antsRegistration tool, FSL (version 5.0.9), AFNI (version 16.2.07), mcflirt, AROMA, R-studio (v.3.6.0 (2019-04-26)) with packages: readxl v. 1.3.1, pheatmap v 1.0.12 and gdata v. 2.18.0, GraphPad Prism8, SAS (v 9.4 for Windows)

For manuscripts utilizing custom algorithms or software that are central to the research but not yet described in published literature, software must be made available to editors and reviewers. We strongly encourage code deposition in a community repository (e.g. GitHub). See the Nature Research guidelines for submitting code & software for further information.

Data

All manuscripts must include a data availability statement. This statement should provide the following information, where applicable:

- Accession codes, unique identifiers, or web links for publicly available datasets
- A list of figures that have associated raw data
- A description of any restrictions on data availability

All statistical parametric images of the fMRI study (including the effect size maps) can be found from NeuroVault: https://neurovault.org/collections/ECURNRON/. The accession number for the RNA-Seq data presented in this article is GEO: GSE113764. Secretin receptor expression in human tissues: Online Biology Gene Portal System (BioGPS) http://ds.biogps.org/?dataset=GSE1133&gene=6344. The data that support the plots within this paper, as well as other findings of this study, are available from the corresponding author (P.N.) upon reasonable request.

Field-specific reporting

Please select the one below that is the best fit for your research. If you are not sure, read the appropriate sections before making your selection.

☒ Life sciences ☐ Behavioural & social sciences ☐ Ecological, evolutionary & environmental sciences

For a reference copy of the document with all sections, see nature.com/documents/nr-reporting-summary-flat.pdf

Life sciences study design

All studies must disclose on these points even when the disclosure is negative.

Sample size	Sample size (n=14) was determined by power calculations based on the BAT GU of participants (n=6) reported in our previous study (Li et al. Cell 2018). Sample size calculation was performed with power 0.8, significance level 0.05 and effect size 0.900 with G*power for Wilcoxon's signed rank matched pairs test. N=15 was decided as the final sample size, in order to account for possible loss of data.
Data exclusions	n=15 subjects were included in PET/CT analysis, one subject was excluded due to discontinuation. n=14 subjects were included in fMRI analysis, one subject was excluded due to non-adherence to prespecified fMRI protocol and two due to scanner failure. n=5 non-fasted BAT biopsies were analysed, one sample was excluded due to inadequate sample quality.
Replication	The PET/CT images of the first seven subjects were analyzed twice by two different investigators, in order to check the reproducibility of results. All statistical analysis on measurements conducted in multiple timepoints was replicated by a second investigator. All other statistical tests were reproduced at a later timepoint by the same person originally conducting the analysis. All mentioned attempts at replication were successful.
Randomization	All subjects received secretin and placebo in a randomized order, in both PET and fMRI studies. Randomized allocation sequences for the order of placebo and secretin interventions were generated with the randomized blocks method, with block size of 6, using SAS (v. 9.4 for Windows). The allocation sequence was generated by the Turku University statistics department, that was not otherwise involved in the study. Participants were assigned to the sequence in order of enrollment, by study personnel enrolling participants into the study. In the fMRI test, food images were shown randomly in one of the four fixed orders of stimulus blocks.
Blinding	The study personel assigning participants to randomization sequences according to order of enrollment were not fully blinded, since the same persons handled participants during study days. Subjects were blinded to placebo and secretin interventions in PET and fMRI studies. According to manufacturer's instructions, secretin pentahydrochloride must be administered immediately after preparation and was therefore prepared at the study center. As this was not an industry sponsored study, double blinding was not feasible due to these technical considerations. All PET/CT image analysis was performed by one investigator, who could not be fully blinded due to the investigator also participating in data collection and handling of study subjects. A second investigator, blinded to the intervention, analyzed the PET/CT images of the first seven subjects in order to check the reproducibility of results. In the fMRI test, subjects were also blinded to the purpose of the test and behavioural outcomes were irrelevant to the study. The investigator conducting the fMRI analysis could not be fully blinded due to them also operating the fMRI sequences during the study days. Blinding was not relevant, because analysis is based on a standardized software. Dietary intake, blood samples and composite satiety scores were analysed by inverstigators blinded to the intervention.

Reporting for specific materials, systems and methods

We require information from authors about some types of materials, experimental systems and methods used in many studies. Here, indicate whether each material, system or method listed is relevant to your study. If you are not sure if a list item applies to your research, read the appropriate section before selecting a response.

Materials & experimental systems

n/a	Involved in the study
☐	☒ Antibodies
☒	☐ Eukaryotic cell lines
☒	☐ Palaeontology and archaeology
☐	☒ Animals and other organisms
☐	☒ Human research participants
☐	☒ Clinical data
☒	☐ Dual use research of concern

Methods

n/a	Involved in the study
☒	☐ ChIP-seq
☒	☐ Flow cytometry
☐	☒ MRI-based neuroimaging

Antibodies

Antibodies used	Primary rabbit polyclonal antibody against SCTR (Sigma-Aldrich, Germany, Cat# HPA007269)
Validation	The anti-SCTR antibody has been validated in the human protein atlas project (Atlas Antibodies Cat# HPA007269, RRID:AB_1856640). Anti-SCTR antibody produced in rabbit, a Prestige Antibody, is developed and validated by the Human Protein Atlas (HPA) project (www.proteinatlas.org). Each antibody is tested by immunohistochemistry against hundreds of normal and disease tissues. These images can be viewed on the Human Protein Atlas (HPA) site by clicking on the Image Gallery link. The antibodies are also tested using immunofluorescence and western blotting. To view these protocols and other useful information about Prestige Antibodies and the HPA, visit sigma.com/prestige. Prestige Antibodies® are highly characterized and extensively validated antibodies with the added benefit of all available characterization data for each target being accessible via the Human Protein Atlas portal. The uniqueness and low cross-reactivity of the Prestige Antibodies® to other proteins are due to a thorough selection of antigen regions, affinity purification, and stringent selection. Every Prestige Antibody is tested in the following ways: • IHC tissue array of 44 normal human tissues and 20 of the most common cancer type tissues. • Protein array of 364 human recombinant protein fragments. Relevant citations: • PMID 7612008 • PMID 7700244 • PMID 24522493 As a technical negative control, consecutive slides were stained without primary antibody in the present study.

Animals and other organisms

Policy information about studies involving animals; ARRIVE guidelines recommended for reporting animal research

Laboratory animals	Male 129S6/SvEv mice at the stage of 12 or 5 weeks, respectively, were used for the fasting experiment and for primary brown adipocyte cell culture.
Wild animals	No wild animals were used in the study.
Field-collected samples	No field collected samples were used in the study.
Ethics oversight	Animal experiments were approved by the German animal wellfare authorities at the district government (approval no. 55.2-1-54-2532-34-2016.)

Note that full information on the approval of the study protocol must also be provided in the manuscript.

Human research participants

Policy information about studies involving human research participants

Population characteristics	Twenty-one healthy Finnish male volunteers participated in this study (35.2 SD 14.4 years old) within normal BMI range (23.6 SD 1.9kg/m2).
Recruitment	Volunteers were recruited through bulletin boards and newspaper announcements. Selection biases were not detected.
Ethics oversight	The GUTBAT study protocol was reviewed and approved by the Ethics Committee of the Hospital District of Southwest Finland. For the BAT secretin receptor expression study conducted on fasted and non-fasted human BAT samples, the (previously reported) study was approved by the ethics committee of the canton of Zurich (NCT03189511).

Note that full information on the approval of the study protocol must also be provided in the manuscript.

Clinical data

All manuscripts should comply with the ICMJE guidelines for publication of clinical research and a completed CONSORT checklist must be included with all submissions.

Clinical trial registration	NCT03290846
Study protocol	The trial protocol and amendment have been provided during submission
Data collection	All participants were recruited and studies were conducted between the years 2016 and 2018. The trial ended when all pre-planned studies were completed. Clinical data were collected and data analysis was conducted at the Turku PET Centre.
Outcomes	The primary outcome measure of the first part of the study was BAT activity, while whole body energy expenditure was listed as a secondary outcome measure. For the second part of the study, brain BOLD activity during palatable vs. non-palatable food image fMRI scans, was listed as the primary outcome measure, while composite satiety score and calorie intake were secondary outcome measures. BAT activity: measured with PET/CT, glucose uptake ([18F]FDG) and perfusion ([15O]H2O) after secretin and placebo infusion. Whole body energy expenditure: indirect calorimetry was collected during PET/CT scans. BOLD activity: measured while subjects viewed palatable vs. non-balatable food images after secretin and placebo infusions. Composite satiety score: measured with a visual analogue scale questionnaire during the study day at prespecified time points. Calorie intake: measured from food eaten after the fMRI scans at the PET Centre

Magnetic resonance imaging

Experimental design

Design type	Task-related fMRI, block design.
Design specifications	12 blocks, 16.2 for each block, no interval between blocks.
Behavioral performance measures	Behavioral outcomes are irrelevant

Acquisition

Imaging type(s)	Functional and structural.
Field strength	3 T
Sequence & imaging parameters	fMRI: TR = 2600 ms, TE = 30 ms, 75° flip angle, 240 mm FOV, 3.0 mm slice thickness, 3 × 3 × 3 mm voxel size, 45 interleaved slices acquired in ascending order without gaps; T1: TR 8.1 ms, TE 3.7 ms, flip angle 7°, 256 x 56 x 176 mm FOV, 1 × 1 × 1 mm voxel size
Area of acquisition	Whole brain scan.

Diffusion MRI ☐ Used ☒ Not used

Preprocessing

Preprocessing software	SPM12 software (www.fil.ion.ucl. uk/spm/); 6 - mm FWHM Gaussian kernel.
Normalization	Echo-planar and structural images were co-registered, the structural images was normalized to the MNI space using linear and non-linear transformations, and the resulting warps were subsequently applied to the functional images.
Normalization template	MIN305
Noise and artifact removal	Head motion was corrected by realigning the images to the first scan by rigid body transformations.
Volume censoring	Realignment parameters were included as nuisance covariates in statistical modeling to account for head motion.

Statistical modeling & inference

Model type and settings	In the fMRI analysis, the whole-brain random effects model was applied using a two-stage process with separate first and second level. This model assesses the effects based on inter-subject variance and allows inferences at the population level. For each participant, GLM was used to predict regional effects of task parameters (palatable and non-palatable foods) and drug condition (secretin, placebo) on BOLD indices of activation. Subject-wise contrast images were generated for the effect of palatable versus non-palatable foods in the secretin and placebo condition and subjected to second-level analyses.
Effect(s) tested	food types (palatable, non-palatable foods) and drug condition (secretin, placebo) on BOLD indices of activation; factorial design

Specify type of analysis: ☒ Whole brain ☐ ROI-based ☐ Both

Statistic type for inference
(See Eklund et al. 2016)

> voxel-wise

Correction

> FDR

Models & analysis

n/a	Involved in the study
☒	☐ Functional and/or effective connectivity
☒	☐ Graph analysis
☒	☐ Multivariate modeling or predictive analysis